Title
THE IMPORTANCE OF INDIRECT TRANSITIONS ON (p,t) REACTIONS ON DEFORMED NUCLEI

Authors
Ascuitto, R.J.
Glendenning, Norman K.
Sorensen, B.

Publication Date
1971-10-01

Submitted to Nuclear Physics

LBL-248
Preprint

THE IMPORTANCE OF INDIRECT TRANSITIONS ON (p, t) REACTIONS ON DEFORMED NUCLEI

R. J. Ascuitto, Norman K. Glendenning,
and B. Sørensen

October 1971

AEC Contract No. W-7405-eng-48

DISCLAIMER

THE IMPORTANCE OF INDIRECT TRANSITIONS ON (p,t) REACTIONS ON DEFORMED NUCLEI

R. J. Ascuitto

Wright Nuclear Structure Laboratory
Yale University
New Haven, Connecticut 06520

Norman K. Glendenning

Lawrence Berkeley Laboratory
University of California
Berkeley, California 94720

B. Sørensen

The Niels Bohr Institute
University of Copenhagen
Copenhagen, Denmark

October 1971

Abstract

The (p,t) reaction on deformed nuclei has been computed with the inclusion of indirect transitions that go through intermediate rotational states. The indirect transitions are almost as large as the direct for the 2^+ state and their inclusion is essential to bring about agreement with the shape and magnitude of the differential cross-section. For the 4^+ state some of the indirect transitions are even stronger than the direct one. The sensitivity of the reaction to β_4 and β_6 terms in the shape has been investigated and found to be weak.

1. Introduction

The mechanism involved in a nuclear reaction is pictured in one of two ways. Either a compound nucleus is formed involving the rapid sharing of the incident energy through many collisions, followed by its eventual decay when sufficient energy again becomes concentrated on one or several particles that they can escape, or a single reaction takes place in which only those nucleons are involved which are needed to change the target ground state into a nearby and closely related final state. The latter reaction, referred to as a direct one, has proved enormously valuable in nuclear spectroscopy since Butler first postulated it to explain the forward peaked angular distributions populating low-lying states in (d,p) reactions. That all nuclear reactions should fit so neatly into one or the other of these very different categories, does seem implausible however. It has been known for some time that the excitation of intermediate states in inelastic scattering is important for deformed nuclei, though not so important for vibrational nuclei, except for any state whose structure forbids or inhibits its direct production in a single interaction (such as 2-phonon states). In the last several years we have been investigating the question of whether higher order processes in nucleon transfer reactions are important[1-8]). The processes which we expect are most important are those in which an excited state is produced by an inelastic collision and is followed by the transfer reaction to the final state, together with these interactions in reverse order. Such processes, when important, will involve inelastic transitions to states which are enhanced, and the final states for which the multiple-step processes are important will be those which have a considerable fraction of their parentage based on such collective excited states. Thus the

spectroscopy of a different class of states is opened up, namely those whose main parent in a collective state as compared to those up till now most extensively studied, which have the target ground state as main parent. Naturally the former states, on average, to appear higher in the energy spectrum, but since the theoretical analysis has until now assumed that any direct reaction proceeds in a single step, undoubtedly many analyses have yielded misleading information.

On way of handling such reactions was suggested by Penny and Satchler[9]), and is a straightforward (though computationally difficult) generalization of the usual DWBA. We have formulated the source term method[1]) which has computational and conceptual advantages, but which is physically equivalent.

Our calculations of the (p,t) reaction on vibrational nuclei suggested that relative cross sections could be changed by almost a factor of two when such multiple-step processes are included[4]). However, the angular distributions in that work were not strongly altered from the usual direct transition, and so it was difficult to confirm the result by experiment, since the structure of the nuclei involved is not so well known that it can be isolated from the reaction mechanism. In (d,p) reactions on deformed nuclei, large effects, up to a factor ten, were found for weakly excited states[5]). The experimental data in these cases was not so extensive as to allow a detailed test of the theory, but was sufficient to indicate that the size of the effect is about right. Very recently we reported what we consider to be the firmest evidence for strong higher-order processes in direct reactions, and the way in which the higher-order processes interfere with the single-step direct transition to bring about agreement with experiment is strong evidence of the correctness of the reaction mechanism[6]).

In this publication we present more details on that work together with more extensive and refined calculations. The reaction under discussion is the (p,t) reaction on deformed nuclei. The inelastic excitation of rotational states can be very accurately described in terms of a macroscopic picture in which the nucleus is allowed to have a shape defined in terms of several multipole deformation constants β_λ (λ = 2,4,6)[10,11]. The rationale is the following: Since the intrinsic structure is not altered by inelastic transitions between members of a rotational band, the nucleus can be thought of as being the source of a deformed field in which the exterior particle scatters. Since only the ground state rotational members will be treated, this field must be an optical potential because all of the other many open channels are omitted from the explicit treatment. The optical potential is a phenomenological representation of a quite definitely defined, though incalculable theoretical construct, which allows one to solve the scattering problem in a subspace of the open channels, in this case the ground state rotational levels.

Although the inelastic transitions can be treated by the above macroscopic picture, an explicit description of the intrinsic structure of the nucleus is needed to describe the (p,t) transitions. Since the higher-order transitions will generally involve a different multipole in the (p,t) reaction than the direct transition, it is important to treat the intrinsic structure, which determines the relative strength of these multipoles, with as high a degree of accuracy as is feasible. For the intrinsic state we adopt a BCS vacuum state of quasiparticles. The quasiparticles in this case are constructed from Nilsson-like states. However since the form of the wave function in the surface and asymptotic regions is very important in reactions, we do not use

Nilsson's oscillator wave functions but instead generate the single-particle states by solving the deformed Woods-Saxon problem, which again is characterized in terms of deformation constants β_λ ($\lambda = 2,4,6$).

The reader not interested in the technical details of the calculation can skip the next three sections. Section 2 describes the coupled equations used to treat simultaneously inelastic transition and (p,t) reactions. The intrinsic structure of rotational states and the (p,t) transfer amplitudes are discussed in sec. 3. Because the nuclear shape enters in the potentials describing three types of particles in this problem, a way of handling the deformation so as to yield a consistant representation of the multipole fields for all particles has to be arrived at, and this is discussed in sec. 4. In sec. 5 it is established that in some cases the higher-order processes are stronger than the direct one usually treated. In sec. 6 and 7 we deal in detail with two reactions at opposite ends of the rare earth region (i.e. for both positive and negative β_4 nuclear shapes). In particular it is demonstrated that the higher-order processes are crucial in obtaining agreement with the data for (p,t) reactions on deformed nuclei. Indeed for higher spin states they dominate the direct transition.

2. Coupled Equations for Inelastic Scattering and Two-Nucleon Transfer

In other publications we have described our method for treating simultaneously, inelastic processes and the two-nucleon transfer reactions[1,3]). Here we shall set down the basic equations for the purpose of discussing their ingredients which are particular to the rotational nuclei treated in this work. In addition to the direct production of the final state in a (p,t) reaction, these equations allow for its indirect production through all the inelastic and reaction transitions connecting the states in both nuclei. The inelastic processes are treated to all orders, but the reactions, which are weaker, are treated only in first order. This accounts for the asymmetry in our equations[12]). The reaction we treat here is

$$p + (A + 2) \rightarrow t + A \quad .$$

For the proton channels these equations are, for each channel p

$$(T_p - E_p)\, v_p^{\pi I}(r) + \sum_{p'} V_{pp'}^{\pi I}(r)\, v_{p'}^{\pi I}(r) = 0 \quad , \tag{1}$$

where matrix elements are taken with respect to the channel wave functions

$$\phi_{p\pi I}(\hat{r}, A + 2) = \left[\mathcal{Y}_{\ell_p s_p j_p}(\hat{r}, \sigma)\, \Phi_{J_p}(A + 2) \right]_I^M \quad . \tag{2}$$

Here $\mathcal{Y}$ is a spin orbit function and Φ is a nuclear wave function. On the left side, p is used to denote the collection of quantum numbers

$$p \equiv \ell_p s_p j_p J_p \quad . \tag{3}$$

In addition V is a complex deformed optical potential which is a parametrization of an effective interaction which enters the problem because of the truncation to a finite system, in this case the low-lying rotational states[10]).

The equations describing the final partition of the system are

$$(T_t - E_t)\, w_t^{\pi I}(R) + \sum_{t'} V_{tt'}^{\pi I}(r)\, w_{t'}^{\pi I}(R) = \sum_p \rho_{p,t}^{\pi I}(R) \quad . \tag{4}$$

Here $\rho_{p,t}$ is a source term representing the appearance in channel t of triton due to a transfer reaction in channel p. If this is evaluated under the assumptions[13]) usually made in two-nucleon transfer theory, it may be written as[3])

$$\rho_{p,t}^{\pi\, I}(R) = \frac{A+2}{A} D_0 \sum_J A_J^I(p,t)\, \tilde{u}_J^{p,t}(R)\, v_p^{\pi I}\left(\frac{A}{A+2} R\right) \tag{5}$$

$$A_J^I(p,t) = (-)^{J_p+I-1/2-J} \left(\frac{\hat{j}_p \hat{j}_t \hat{\ell}_p \hat{\ell}_t \hat{J}_p \hat{J}}{4\pi}\right)^{1/2} \begin{pmatrix} \ell_p & J & \ell_t \\ 0 & 0 & 0 \end{pmatrix} \times \begin{Bmatrix} \ell_p & \ell_t & J \\ j_t & j_p & 1/2 \end{Bmatrix} \begin{Bmatrix} j_p & j_t & J \\ J_t & J_p & I \end{Bmatrix} \quad . \tag{6}$$

In the above equation D_0 is a constant which effects the overall normalization of the (p,t) cross sections, but not their relative values. The functions $\tilde{u}_J^{p,t}$ are discussed in the next section and are intimately connected with the internal structure of the nuclei, while v_p is a solution to the system (1).

The system of eqs. (1) and (4) must be solved for each parity π and angular momentum I, up to some maximum value which yields convergence in the cross sections. The boundary conditions which are to be imposed on the solutions have been specified elsewhere, as has the construction of the scattering amplitude from the S-matrix elements which are obtained from the asymptotic behavior of w_t[1,3]).

As mentioned in the introduction, the inelastic transitions which enter this calculation through the matrix elements of a complex optical potential V in (1) and (4) are treated as macroscopic excitations of a rigid rotor. The matrix elements of V with respect to the channel functions ϕ_p or ϕ_t (eq. 2) can be calculated as a straightforward extension from spin 0 to spin 1/2 projectiles along the lines given in ref. 10 for spin 0.

3. Nuclear Structure and the Two-Nucleon Transfer Amplitudes

We adopt the Bohr-Mottelson adiabatic hypothesis in order to write the wave function for the ground band members of (A + 2) as

$$\Phi^{M}_{J_p} = \left(\frac{\hat{J}_p}{8\pi^2}\right)^{1/2} D^{J_p}_{MO} \; X_o(A+2) \qquad (7)$$

and a similar function for (A). Here $\hat{J} = 2J + 1$, D^J is a rotational function, and $X_o(A + 2)$ is the intrinsic wave function which describes the motion of the nucleons inside the deformed nucleus.

The (p,t) transitions between various rotational states of (A + 2) and (A) are determined by the structure of the intrinsic states of these nuclei, and this information can be most compactly expressed through a set of parentage factors [13]. These are the amplitudes for finding in the state J_p of the nucleus (A + 2), a neutron pair in the single-particle states a and b with angular momenta coupled to LSJ, given that the remaining A nucleons are in a state of motion corresponding to the state J_t of the nucleus (A). These parentage amplitudes can be expressed as[3])

$$\beta_{(ab)LSJ}(J_p, J_t) = [\hat{J}_p(1 + \delta_{ab})]^{-1/2} \langle J_p \| [d^+_a d^+_b]^{Lab}_{LSJ} \| J_t \rangle \qquad (8)$$

Here d^+_a creates a particle in the state whose quantum numbers we denote by a. Using the wave functions eq. (7), and transforming the pair creation operator into the <u>intrinsic</u> frame, we find

$$\beta_{(ab)LSJ}(J_p, J_t) = (1 + \delta_{ab})^{-1/2} \; (-)^J \; C^{J_p \; J \; J_t}_{0 \; 0 \; 0} \langle X_o(A+2) | [d^+_a d^+_b]^{intr}_{LSJ} | X_o(A) \rangle \qquad (9)$$

Note the factorization into a Clebsch-Gordan coefficient depending on the spins of the particular members of the bands and a matrix element depending only on the intrinsic structure of the two nuclei. Accordingly we define the intrinsic parentage factors as

$$\beta^{intr}_{(ab)LSJ} = (1 + \delta_{ab})^{-1/2} \langle X_o(A+2) | [d^+_a d^+_b]^{intr}_{LSJ} | X_o(A) \rangle \ . \qquad (10)$$

Of course, the intrinsic structure of the nuclei determines the strength of the various multipoles of the transfer, as eq. (10) expresses. Considerable care must therefore be taken in constructing the intrinsic wave functions if these strengths are to be correctly described. We use BCS wave functions to describe the intrinsic wave functions X_o. The single-particle wave functions from which X_o is constructed are eigenfunctions of a deformed Woods-Saxon potential having a shape defined by three deformation parameters β_2, β_4, β_6.

One is free to choose the single particle representation a,b as a matter of convenience. The harmonic oscillator forms a very convenient representation because of the existence of the Talmi-Moshinsky transformation to relative and center of mass coordinates. Therefore we use this representation, so that $a \equiv n_a \ell_a$. In any case one can construct from the above amplitudes, a set of two-neutron wave functions Ψ whose physical significance can be inferred from the definition given above for β:

$$\Psi_{LSJ}(1,2) = \sum_{a \leq b} \beta^{intr}_{(ab)LSJ} [\psi_a(1) \psi_b(2)]_{LSJ} \qquad (11)$$

Here ψ_a is a single-particle wave function of the chosen representation. However, only that part of the motion of the two neutrons described by Ψ which overlaps with the triton internal wave function is effective in the (p,t) reaction. Employing a Gaussian form for the triton wave function as in ref. 13, the relevant projection is

$$\left\langle \frac{1}{\sqrt{4\pi}} u_{10}(3\eta^2 r^2)\, \chi_0(\sigma_1, \sigma_2) \,\middle|\, \Psi_{J0J}(1,2) \right\rangle = \tilde{u}_J(R)\, Y_J(\hat{R}) \qquad (12)$$

where u_{10} is the ^1S oscillator function defined there, and χ_0 is a singlet spin function.

According to eq. (9) and (10), the projected wave functions for the transition connecting the state J_t to J_p, which appear in the source term eq. (5) are

$$\tilde{u}_J^{p,t}(R) = C \begin{matrix} J_p & J & J_t \\ o & o & o \end{matrix} \tilde{u}_J(R) \quad . \qquad (13)$$

The physical significance of the projected wave functions, $\tilde{u}_J(R)$ is the following. They describe how the center of mass of the neutron pair moves in the intrinsic state of the nucleus (A + 2) when their correlation in spin and space corresponds to what it is in the triton (^1S), given that the remaining A nucleons are in a state of motion corresponding to the intrinsic structure of (A).

If the cross section for the direct transition from the ground state to the rotational state of spin J were computed in the DWBA, they would occur in the familiar matrix element

$$T_{0 \to J} \propto \int \psi_t^{(-)*}(R)\, \tilde{u}_J(R)\, Y_J(\hat{R})\, \psi_p^{(+)}(\underset{\sim}{R})\, d\underset{\sim}{R} \qquad (14)$$

where the usual zero-range interaction has been employed.

For the reaction ^{176}Yb(p,t)^{174}Yb the projected functions $\tilde{u}_J$ are shown in fig. 1 for the lowest four multipoles. In fact all even multipoles exist, but as can be seen, the higher ones become smaller. (We have computed them up to J = 12 and include all these in the calculations. The J = 12 may contribute, for example, to the transfer between the two 6^+ members of the two nuclei).

This calculation was done in the following approximate way. The shape of ^{176}Yb was taken from the alpha scattering analysis. The single-particle wave functions in a Woods-Saxon potential having this shape were computed. The same wave functions were used for ^{174}Yb. The BCS vacua of quasiparticles was computed in each nucleus from the resulting spectrum with a pairing force of appropriate strength, as we discuss later. The parentage amplitudes were computed from the innocent looking expression, eq. (10), and the projected wave functions then computed from eq. (12) as described in more detail in the appendix.

Taking into account that the region of greatest importance in the (p,t) reaction is in the region $r \gtrsim 7F$ (because of the absorption), the main features to note are that the J = 0 transition is the most probable with the others decreasing in importance as J increases. This can be understood since these functions express the amplitude that all of the rotational motion is carried by the transferred pair, and this ought to become less likely as J increases.

4. Consistent Treatment of the Nuclear Shapes

The shpae of a number of rare earth nuclei have been determined through a careful analysis of alpha inelastic scattering[11]). The nuclei were treated as rigid rotors which interact with the alpha particle through a deformed optical potential, whose shape was specified by

$$R = R_\alpha \left[1 + \sum_{\gamma=2}^{6} \beta_\lambda^\alpha \, Y_{\lambda_o}(\theta) \right] \quad . \tag{15}$$

The deformation constants β_λ^α must be subjected to some interpretation before being used for other purposes because they are associated with the optical potential radius R_α. We consider the inelastic experiments to have determined the strengths of the multipole fields relative to each other since the deformation always occurs together with the nuclear size in the product $R\beta$ in the expression of the multipoles of the deformed field[10]).

The present problem involves the interaction of three different types of particles with the nucleus, the triton, proton and bound neutron, and thus involves three different optical potentials. It is not clear, either from experiment or theory, whether the nucleus appears to have the same "shape" to each particle. In any case, there is an underlying nuclear shape defined by the shape of the mass density,

$$R(\theta) = cR_\rho \left[1 + \sum_{\lambda=2}^{6} \beta_\lambda \, Y_{\lambda_o}(\theta) \right] \quad . \tag{16}$$

(Here c is merely a constant which depends upon β_λ and insures that the volume contained by the deformed shape $R(\theta)$ equals that of the sphere of radius R_ρ.)

We use for the mass density radius, R_ρ, values determined by Myers from a Thomas-Fermi treatment of the nucleus in which agreement between the charge density and electron scattering experiments was required[14]).

The deformation constants for the density, β_λ, were scaled from tabulated values in the alpha analysis[11]) according to

$$cR_\rho\beta_\lambda = R_\alpha\beta_\lambda^\alpha \quad . \tag{17}$$

Then we write the radius of the optical potential for particle k (k = p, t, or n) as

$$R_k(\theta) = r_k + cR_\rho \left[1 + \sum_{\lambda=2}^{6} \beta_\lambda Y_{\lambda_o}(\theta)\right] \quad . \tag{18}$$

That is to say, to the density radius of the nucleus we add a constant r_k, which can be thought of as an effective interaction radius for the scattered particle, due to the nature of the effective interaction and the finite size of the particle and it is chosen so that $r_k + R_\rho$ equals the optical model radius for particle k, listed in Table 2. (We note parenthetically that $R_\rho \simeq 1.12\ A^{1/3}$.) The radii of both real and imaginary parts are treated in this way.

Our view is that the deformation of the potential felt by a particle in the vicinity of a deformed nucleus has as its origin the shape of the mass distribution of the nucleus. This is a plausible assumption which is not likely to be far from the truth. The values of the radius and shape parameters are listed in Table 1.

5. Indirect Transitions are Important

In figs. 2 and 3 we show the (p,t) cross sections for two nuclei. One is the spherical nucleus Pb^{15}) and the other the deformed nucleus Yb^{16}). The proton energy is close to the same in both nuclei, and the differential cross section to the 0^+ are similar both in experiment and calculation. However, the 2^+ experimental cross section in the deformed nucleus is markedly different from the corresponding calculations and the results in Pb and in this sense is anomalous.

The reason for this result is that in the deformed nucleus the two indirect transitions that go through the 2^+ in the target nucleus, and the 0^+ in the final nucleus are as strong as the direct first-order transition treated by the DWBA as was shown in our earlier publication[6]). The interference among the three major contributions to the cross section is destructive and results in the reduction in the observed cross section as compared to the direct transition, and a strongly altered angular distribution.

The cross sections that would result from these three routes are shown in fig. 4 if each alone were operative, illustrating the surprising fact that the direct route is not stronger than the two indirect ones shown. In the complete calculation shown in fig. 5 it is seen that the interference brings about the agreement with the "anomalous" observed cross section. That the complete cross section results from the interference of three amplitudes of comparable strength, each different from experiment but which, when interfering, bring about the agreement shown, we consider to be very convincing evidence of the validity of these calculations, and is a decisive statement as to the importance that second order transfer processes can assume.

To see whether this is an energy-dependent effect we have repeated the calculation at 55 MeV and see in fig. 6 again that the direct route does not dominate the two most favoured indirect ones. The interference again reduces the final cross section shown by the dotted curve.

In the case of the 4^+ state, there are many routes of comparable magnitude, which follows from the fact that the strength of the various multipole transitions in both inelastic and reaction channels (see fig. 1) fall off as the multipole increases. Thus, for example, $0_p \rightarrow 2_p \rightarrow 4_t$ and $0_p \rightarrow 4_p \rightarrow 4_t$ are comparable because the dominate multipoles involved are J = 2 and 2 in the first case and 4 and 0 in the second case. The J = 2 is stronger than the J = 4 but weaker than the J = 0. Cross sections for the 4^+ state corresponding to some of the individual routes are shown in fig. 7. Note that the direct transition is much weaker than the indirect ones. Again, comparing with fig. 5, we see that there is a destructive interference which reduces the cross section that would correspond to the direct transition alone. Fig. 8 shows that the above discussion holds also at 55 MeV.

For the 0^+ state the higher-order routes are weaker than the direct, corresponding to the fact that the direct transition is monopole, while the others involve higher multipoles (see fig. 2). The other routes reduce the final cross section, but do not strongly modify the shape characteristic of the direct one.

6. The ^{176}Yb(p,t) Reaction

The calculations reported in the previous section use average proton optical model parameters interpolated in mass and energy from the study of Becchetti and Greenlees[18]. While these parameters reproduce the inelastic proton data for Yb fairly well, as seen in fig. 9, another set which yields the improved fit shown is used throughout the remainder of this paper (except where noted) and are given in Table 2. It turns out that these latter yield also better results for the (p,t) reaction.

For triton parameters we have used those of Flynn et al.[20] based on an analysis at E = 20 MeV and extrapolated in energy according to the reasonable guess below.

$$V = 167 - 0.33\ (E-20)\ \text{MeV}$$

$$W = 37.5 - 127.4\ \left(\frac{N-Z}{A}\right)\ \text{MeV}$$

$$W_D = 0$$

$$r_V = 1.16,\ r_W = 1.498\ \text{F}$$

$$a_V = .752,\ a_W = .817\ \text{F}$$

For the Coulomb radius we choose to use Myer's Thomas-Fermi formulas which yield $r_c \sim 1.123$ and reproduce the charge radii observed in electron scattering[14].

At this point we state our philosophy concerning optical model parameters to be used in a coupled-channel calculation. It is supported both by our understanding of the structure of the optical potential[10], and experience[21]. Both spherical and deformed nuclei, contain in common, intrinsic particle excited states which are not identical, but which in their multiplicity at higher excitation, will contribute rather similarly to the optical potential. Were it not

for the rotational states of the deformed nucleus, the one-channel optical potential for nearby spherical and deformed nuclei would therefore be similar. However, the strongly coupled rotational states cause large changes in the one-channel optical potential of nearby spherical and deformed nuclei [21]). However, when the rotations are treated explicitly in a coupled-channel treatment, then it is expected, and indeed born out in practice [21]), that since now in both cases the optical potential must take care only of the intrinsic excitations and reactions that are roughly common to both spherical and deformed nuclei (especially since the optical potential is dominated by the high-energy region of dense states), the same, or a very similar optical potential should apply to both a spherical nucleus and a neighbouring deformed one in which the rotations are treated explicitly. For this reason we use, in our coupled-channel calculations, optical parameters that are characteristic of spherical nuclei.

In an effort to diminish the number of parameters, the calculation reported in sec. 5 employed pairing gaps obtained by the Nilsson-Prior prescription [22]) yielding Δ_n = .55 and .6 MeV for ^{176}Yb and ^{174}Yb. That prescription may fail in case of low density of single-particle levels. A proposed gap in the neutron spectrum at ^{176}Yb may suggest the use of a Δ_n that is smaller than predicted by the Nilsson-Prior formula. In order to accommodate this evidence and at the same time obtain a smooth transition to the more neutron deficient Yb-isotopes we used in the calculation presented in this section Δ_n = 0.36 MeV for ^{176}Yb and Δ_n = 0.575 MeV for ^{174}Yb.

A complete calculation of the ^{176}Yb(p,t) reaction which now includes the 6^+ state and the new optic and gap parameters is shown in fig. 10 where the

agreement is rather good for all states. We emphasize that the cross sections are plotted according to their relative values so that we have achieved agreement in both magnitude and angular distribution. The deformation constants β_2, β_4, β_6 are based on those obtained in an analysis of α-elastic scattering as discussed in sec. 4.

To determine if the (p,t) reaction is a good means of determining β_4, as has been established for α-inelastic scattering[11]), we set $\beta_4 = \beta_6 = 0$ and choose a value for β_2 which yields the same quadrupole moment as for the calculation of fig. 10 with all three values for β_4 finite. This choice for β_2 insures that the 2^+ inelastic cross section will be about the same in both cases. The resulting (p,t) cross sections are shown in fig. 11 and we see that while the details of the 4^+ cross section are altered, the magnitude is about the same thus negating the procedure used by Kubo et al.[17]) based on a comparison of the relative 0^+ and 4^+ integrated cross sections. It is clear from figs. 10 and 11 that the (p,t) cross sections are not especially sensitive to higher-order deformations as contrasted with α-inelastic scattering which is highly sensitive. Figure 12 makes the same comparison at 55 MeV (these calculations are based on the optical parameters of Bechetti and Greenlees[18]). We reach the same conclusion as for the lower energy.

In the BCS calculation of the nuclear ground state structure, there is an arbitrariousness associated with the number of levels to be used. All the above calculations used 20 levels. We have also done a calculation using 40 levels, and with a pairing strength adjusted to yield the same gap as for the 20-level case. The effect on the (p,t) cross section, shown in fig. 13, is that the 0^+ and 2^+ states are given too much strength compared to the 4^+ and 6^+

(the same overall normalization is used as for fig. 10). The relative strength in different multipoles thus roughly determines the number of levels over which the assumption of a constant pairing strength is valid. This conclusion has not been reached in the literature before, based on other kinds of data.

To contrast the excellent agreement shown in fig. 10, where all inelastic and transfer transitions are included, we show in fig. 14 two DWBA calculations, which include just the direct transitions from the target ground state. The solid curves represent the standard type of DWBA calculation in the sense that the optical parameters were adjusted so that they reproduced the elastic proton and triton cross sections computed in the coupled-channel calculations. That is to say, we are using the coupled-channel elastic cross sections in lieu of data. However, as seen in fig. 9, the proton data is reproduced. It was then necessary to use an overall normalization for the reaction that is three times smaller than used in the complete calculation of fig. 10, corresponding to the fact, already emphasized, that the higher-order processes acting with the direct, reduce the cross sections. We have to consider it fortuitous that the σ_4/σ_0 ratio comes out roughly correctly, since this is not true of σ_2/σ_0 or σ_6/σ_0, thus again speaking against the procedure used by other authors to extract β_4 from the (p,t) cross section on the basis of a DWBA calculation of this ratio[17,19]). In fact as seen in fig. 7, the direct route, on which their analysis was based, has a smaller amplitude than the higher-order ones. The dashed curves correspond to the same optical parameters as used in the complete coupled-channel calculation of fig. 10 and again illustrates the unreliability of the DWBA calculation with another set of parameters as contrasted with the complete calculation.

7. Another Example: ^{154}Sm(p,t)

Whereas Yb has a negative value for β_4, we now study a reaction, ^{154}Sm(p,t) in which the nuclei have positive β_4. Again the intrinsic nuclear state was obtained as described in sec. 3, with pairing gaps of 1.022 and 0.997 MeV for ^{154}Sm and ^{152}Sm. Again we exhibit in fig. 15 two DWBA calculations with overall normalization (i.e. each set of curves has a common normalization) chosen to roughly agree with the data. It is 2.5 times smaller than the complete calculation discussed next, again corresponding to the fact that the higher-order processes reduce the cross sections that would result from the direct transitions acting alone. We see that the relative cross sections to the 2^+ and 4^+ states are very badly reproduced as are the angular distributions. In contrast, the complete calculations which includes the higher-order processes, is shown in fig. 16, and now the relative cross sections and angular distributions are very well reproduced. The angular distribution for the 2^+ state has been greatly altered from the shape of the direct route, by the other routes.

As before, to test whether there is a sensitivity to β_4, we have set $\beta_4 = \beta_6 = 0$ and adjusted β_2 so that the quadrupole moment and thus the strength of the 2^+ inelastic transition is about the same as in the complete calculation of fig. 16. These results are shown in fig. 17. While there is some change in angular distribution, it is clear from a comparison of the figures that this reaction is not nearly so sensitive to the value β_4 as the α-inelastic scattering, and as for Yb, we find that the behavior of the relative integrated cross sections σ_4/σ_0 with respect to β_4 as predicted by Kubo et al.[17]) would not yield accurate values β_4.

8. Summary

We have computed the effects of higher-order processes on the (p,t) reaction on deformed nuclei. There is much evidence from various sources that the rotational model provides a good description of these nuclei. This implies the existance of an intrinsic state from which all two-nucleon transfer amplitudes to the ground band of the neighboring nucleus can be computed. This is in contrast to spherical nuclei where the various states of different spin are independent of each other. We may thus have a high degree of confidence that relative cross sections can be computed correctly if the reaction mechanism is properly treated. This indeed turns out to be the case where, with an accuracy unprecedented in reaction theory, the cross sections to the 0^+, 2^+, 4^+ and 6^+ members of the ground band are reproduced. However, this comes about only because the many higher-order routes of producing these states were included in the calculation. Especially for the higher spins, the higher-order processes were more important than the first-order ones, traditionally treated by the DWBA. In some cases, and most dramatically for the 2^+ state, the interference among the various ways of producing a state, strongly alters the cross section computed in DWBA. In both cases we studied, i.e. in a nucleus near both ends of the rare earth region (i.e. both positive and negative β_4) and at two different energies, the interference was destructive but of different magnitude for each state in a given nucleus, and also different in the two nuclei for the same spin state. The interference of the various routes, which was between amplitudes of comparable magnitude, did however bring about the remarkable agreement mentioned, and is the strongest confirmation that higher-order processes in transfer reactions are of importance for a correct description, and that they

can be computed with satisfactory accuracy. This success supports the conclusions that we reached elsewhere[4]) for spherical nuclei, where however direct confirmation from experiment was not possible, both because of the lack of data, and the fact that the nuclear structure information was more tenuous. We claim therefore on the basis of this work that we have demonstrated that our calculation of higher-order processes is correct, and on the basis of that other work, that they are important in spherical nuclei, though less dramatic in producing changes in angular distributions computed for the direct transition.

Naive considerations had led earlier to the conclusion that second-order processes must be weak unless the first-order is nearly forbidden. In an earlier letter[6]), however, we pointed out that the probability for multiple-step processes is given by the product of conditional probabilities and not disjoint probabilities which was the basis of earlier arguments against multiple-step processes. The reader is referred to that letter for details.

The most notable features of the DWBA calculations are that the relative cross sections are grossly incorrect and for several states, most notably the 2^+, so was the angular distribution. We understand that the reason for this is that the higher-order processes play such an important role and indeed for some states are stronger than the direct one treated by the DWBA. The question may occur to some readers whether there is a prescription by which the optical model parameters in the DWBA calculation could be modified so as to retrieve agreement. We are convinced that the answer is negative. The interference is of different magnitude for different states and alters angular distributions drastically in some cases and not in others. The underlying theory of the optical potential moreover offers no hope. It is a construct

which can reproduce on any one channel (in practice the elastic) the effects of all the others. This then determines it, and it has no meaning outside this one channel space if strong coupling effects are explicitly acting.

We emphasize that at each step of the calculation we made the physically reasonable choices of parameters and had we not been rewarded with success, we would not have known what else to try.

Contrary to suggestions made elsewhere[17,19], it seems to us that the (p,t) reaction is not a good way of determining higher multipoles in the nuclear shape. This suggestion was made on the assumption that the reaction could be described by its direct transition alone. As we have seen, the direct transition to the 4^+ state, from which it might be hoped to determine β_4 is <u>smaller</u> than many of the higher-order processes. The higher-order processes, since they go through an intermediate state, involve, dominantly, <u>lower</u> multipoles than the direct. Thus sensitivity to higher multipoles in the shape is weak.

Appendix

In this work we obtained the solutions to the single-particle Hamiltonian containing a deformed Woods-Saxon potential given by

$$V = V_o/[1 + \exp \frac{r - R(\theta)}{a}] \qquad (A.1)$$

with $R(\theta)$ defined by eq. (18). They are obtained by diagonalizing the Hamiltonian on an Harmonic Oscillator basis having an extent $N \equiv 2(n-1) + \ell \leqslant 15$ which provides a very accurate description in the surface and out into the tail region. More particularly, the basis functions are expressed in the uncoupled scheme

$$d^+_{k\Omega}|0\rangle \equiv |k\Omega\rangle = \sum_{n\ell\Lambda\Sigma} A^{k\Omega}_{n\ell\Lambda\Sigma}|n\ell\Lambda\rangle \; |1/2\Sigma\rangle \qquad (A.2)$$

for the k'th eigenfunction having projection Ω on the nuclear symmetry axis. Here $|n\ell\Lambda\rangle$ is the oscillator function and spherical harmonic and $|1/2\Sigma\rangle$ the spin function. The multipole fields of the potential (A.1) are computed as in ref. 10 to 8th order in the deformation constants β_2, β_4, β_6, and multipoles up to 8 are retained.

Having obtained the eigenfunctions and eigenvalues in this way, the BCS ground state of quasiparticles is generated using, for most of our calculations 20 levels, in the vicinity of the Fermi level. The transformation between the particles $d^+_{k\Omega}$ and quasiparticles is expressed as

$$d^+_{k\Omega} = U_{k\Omega}\, \alpha^+_{k\Omega} + V_{k\Omega}\, (-)^{1/2-\Omega}\, \alpha_{k-\Omega}$$

where U and V (defined as positive) are solutions of the BCS equations. After a cumbersome calculation, the projected wave functions of eq. (12) can be written as

$$\tilde{u}_J(R) = \sum_N G_{NJOJ} \; u_{NJ}(2\nu R^2)$$

where u_{NJ} is a harmonic oscillator function as defined in ref. 13 and G_{NJOJ}, the structure amplitude for S = 0 transfer, is given by

$$G_{NJOJ} = \sum_{n\ell n'\ell'}{}' \frac{2}{1 + \delta_{nn'}\delta_{\ell\ell'}} \sum_{\Lambda \geq 0} (-)^{\Lambda} C^{\ell \; \ell' \; J}_{\Lambda \; \Lambda \; 0} \; \Omega_\nu$$

$$\langle \nu 0 NJ; J | n\ell n'\ell'; J \rangle \sum_{k\Omega>0}{}' A^{k\Omega}_{n\ell\Lambda} A^{k\Omega}_{n'\ell'\Lambda} U_{k\Omega}(A) V_{k\Omega}(A+2)$$

and exists only for J = even. The prime on the sum indicates that $n\ell$ and $n'\ell'$ do not repeat each other, while the overlap Ω_ν involving the triton and nuclear size parameters is defined in ref. 13. The bracket $\langle \; | \; \rangle$ is a Moshinsky transformation and ν is fixed by the value of the other indices in it.

Footnotes and References

1. R. J. Ascuitto and N. K. Glendenning, Phys. Rev. 181, 1396 (1969).
2. N. K. Glendenning, Proceedings of the International Conference on the Properties of Nuclear States, ed. by M. Harvey (University of Montreal Press, Montreal, 1969).
3. R. J. Ascuitto and N. K. Glendenning, Phys. Rev. C 2, 415 (1970).
4. R. J. Ascuitto and N. K. Glendenning, Phys. Rev. C 2, 1260 (1970).
5. R. S. Mackintosh and N. K. Glendenning, Nucl. Phys. A168, 575 (1971).
6. R. J. Ascuitto, N. K. Glendenning and B. Sørensen, Phys. Letters 34B, 17 (1971).
7. T. Tamura, D. R. Bes, R. A. Broglia and S. Lansdowne, Phys. Rev. Letters 25, 1507 (1970) and errata ibid. 26, 156 (1971).
8. R. J. Ascuitto, N. K. Glendenning and B. Sørensen, Nucl. Phys. A170, 65 (1971).
9. S. K. Penny and G. R. Satchler, Nucl. Phys. 53, 145 (1964).
10. N. K. Glendenning, Proceedings of the International School of Physics "Enrico Fermi", Course XL, 1967, ed. by M. Jean (Academic Press, New York, 1969).
11. D. L. Hendrie, N. K. Glendenning, B. G. Harvey et al., Phys. Letters 26B, 127 (1968).
12. However, if it is believed that the reaction is not weak, the appropriate source term can be added in the initial partition to account for reentrance into this partition from another partition as in ref. 8.
13. cf. N. K. Glendenning, Phys. Rev. 137, B102 (1965).
14. W. D. Myers, Nucl. Phys. A145, 387 (1970).

15. The data was communicated from the Yale Group by D. A. Bromley.

16. The data was communicated by the Minnesota group: M. Oothoudt, University of Minnesota and M. Oothoudt, N. M. Hintz and P. Vedelsby, Phys. Letters 32B, 270 (1970).

17. K. Kubo, R. A. Broglia, C. Riedel and T. Udagawa, Phys. Letters 32B, 29 (1970).

18. F. D. Becchetti, Jr. and G. W. Greenlees, Phys. Rev. 182, 1190 (1969), see eq. (8) of this reference.

19. R. A. Broglia, C. Riedel and T. Udagawa, Nucl. Phys. A135, 561 (1969).

20. E. R. Flynn, D. D. Armstrong, J. G. Beery and A. G. Blair, Phys. Rev. 182, 1113 (1969).

21. N. K. Glendenning, D. L. Hendrie and O. N. Jarvis, Phys. Letters 26B, 131 (1968).

22. S. G. Nilsson and O. Prior, Mat. Fys. Medd. Dan. Vid. Selsk. 32, No. 16 (1961), see eq. (44).

Table 1.

		r_ρ	β_2	β_4	β_6	r_c	β_2	β_4	β_6
^{176}Yb	a	1.124	0.295	-0.0517	-0.0064	1.125	0.328	-0.0635	-0.007
	b	1.124	0.2819	0	0	1.125	0.318	0	0
^{154}Sm	a	1.118	0.29	0.058	-0.019	1.122	0.359	0	0
	b	1.118	0.3048	0	0	1.122	0.359	0	0
^{152}Sm	a	1.117	0.266	0.052	-0.013	1.123	0.314	0	0

The mass and charge radii r_ρ and r_c are taken from ref. 14. The deformation constants under "a" are scaled from ref. 11 according to eq. (17) for reasons discussed there. Under "b" we list a value of β_2 with $\beta_4 = \beta_6 = 0$ which yields about the same strength for the 2^+ inelastic transition as the parameters listed under "a". The deformations of ^{174}Yb are so close to ^{176}Yb that they were taken the same. Since the calculation using parameters "b" was taken to illustrate sensitivity or lack of it to β_4 and β_6, for ^{152}Sm, the same parameters as listed under ^{154}Sm "a" were used for the calculation of type "b".

Table 2. Optical Model Parameters for the 19 MeV (p,t) Reaction. The proton parameters listed under CC (coupled channel) were used for both Yb and Sm. Triton parameters for the CC calculation are given in the text of section 6. Parameters labelled "elastic" reproduce the elastic cross section obtained in the CC calculation (which for protons corresponds well with experiment. For tritons the data is not available).

	V	W	W_D	R_V	R_W	R_C	A_V	A_W	V_s	R_s	A_s
					Protons						
CC	-55.6	0.	-17.8	1.25	1.25	1.125	0.72	0.47	-6.2	1.01	0.75
					Protons + ^{176}Yb						
elastic	-49.652	0.	-21.046	1.309	1.236	1.125	0.713	0.557	-6.2	1.01	0.75
					Tritons + ^{174}Yb						
elastic	-247.757	-13.571	0.	0.938	1.346	1.125	0.846	1.141	——	——	——
					Protons + ^{154}Sm						
elastic	-55.158	0.	-21.562	1.219	1.188	1.125	0.776	0.570	-6.2	1.01	0.75
					Tritons + ^{152}Sm						
elastic	-254.685	-17.057	0.	0.964	1.254	1.123	0.724	1.267	——	——	——

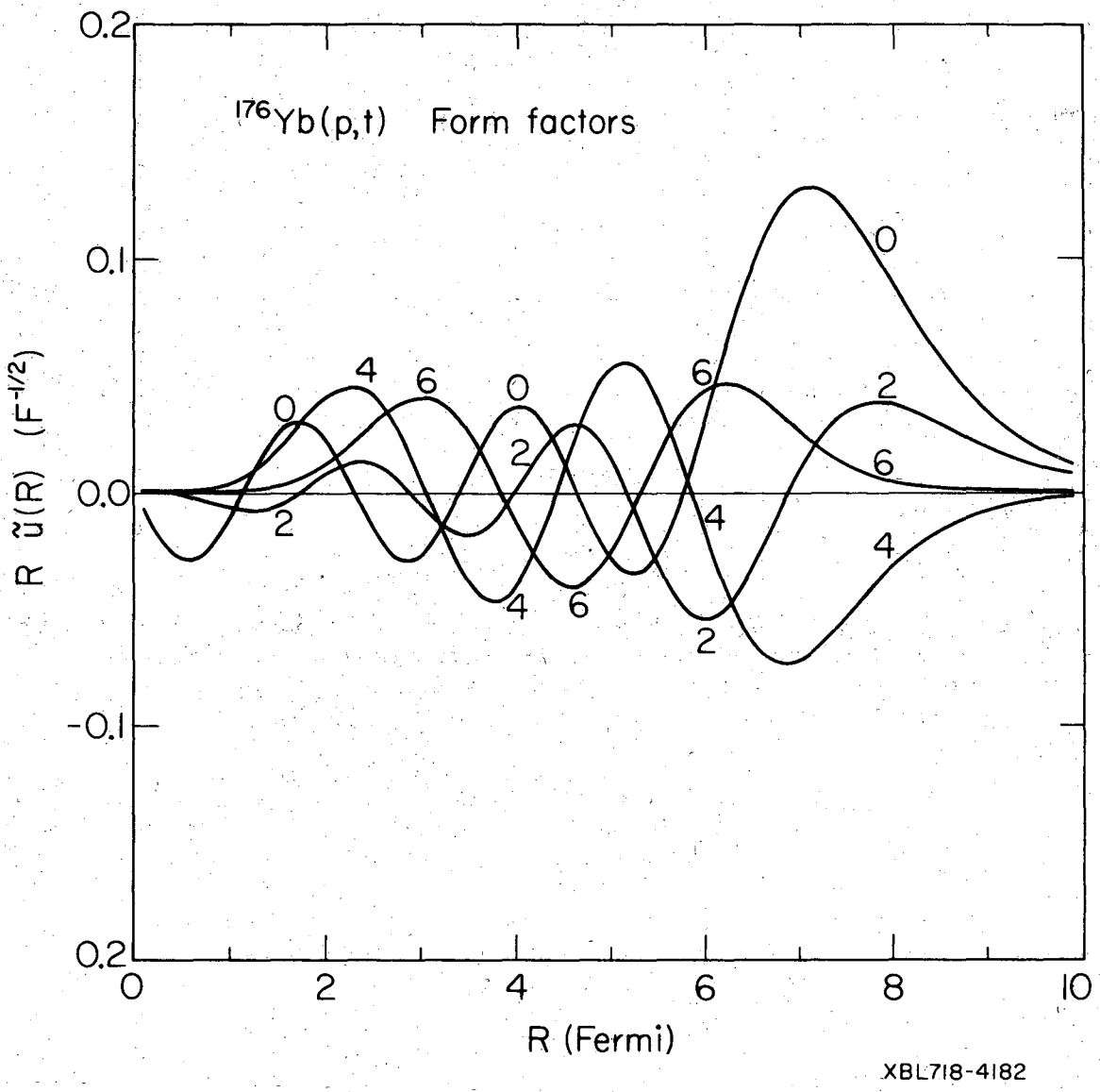

Fig. 1. The projected wave functions or form factor that show the strength (determined mainly by the surface region) of the various multipoles for transferring a pair of particles between ground state members of the rotational nuclei ^{176}Yb and ^{174}Yb.

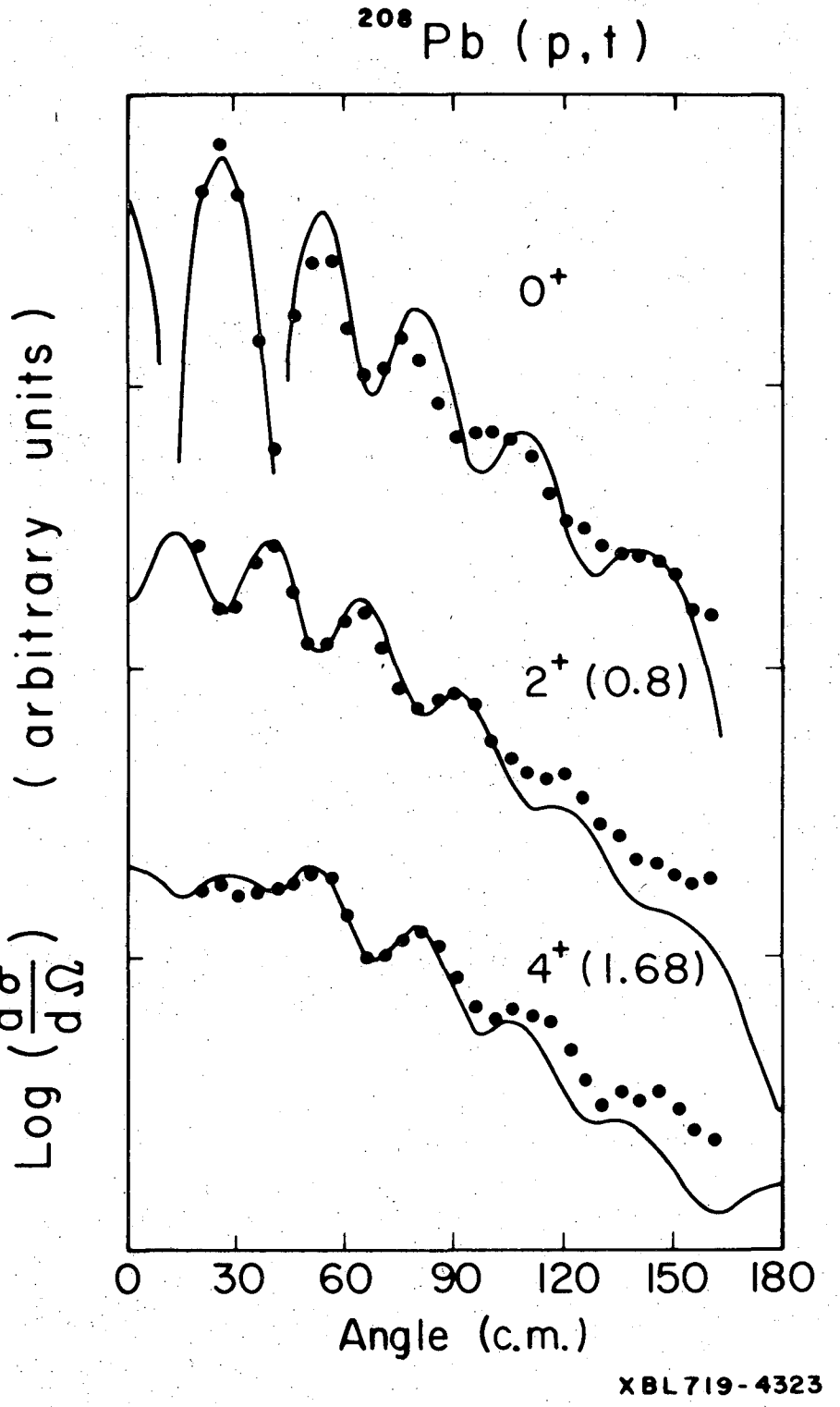

Fig. 2. Angular distributions to the lowest states in ^{206}Pb at 22 MeV. The calculated DWBA cross sections are adjusted in magnitude relative to the ground state by 15% for the 2^+ and 20% for the 4^+ state.

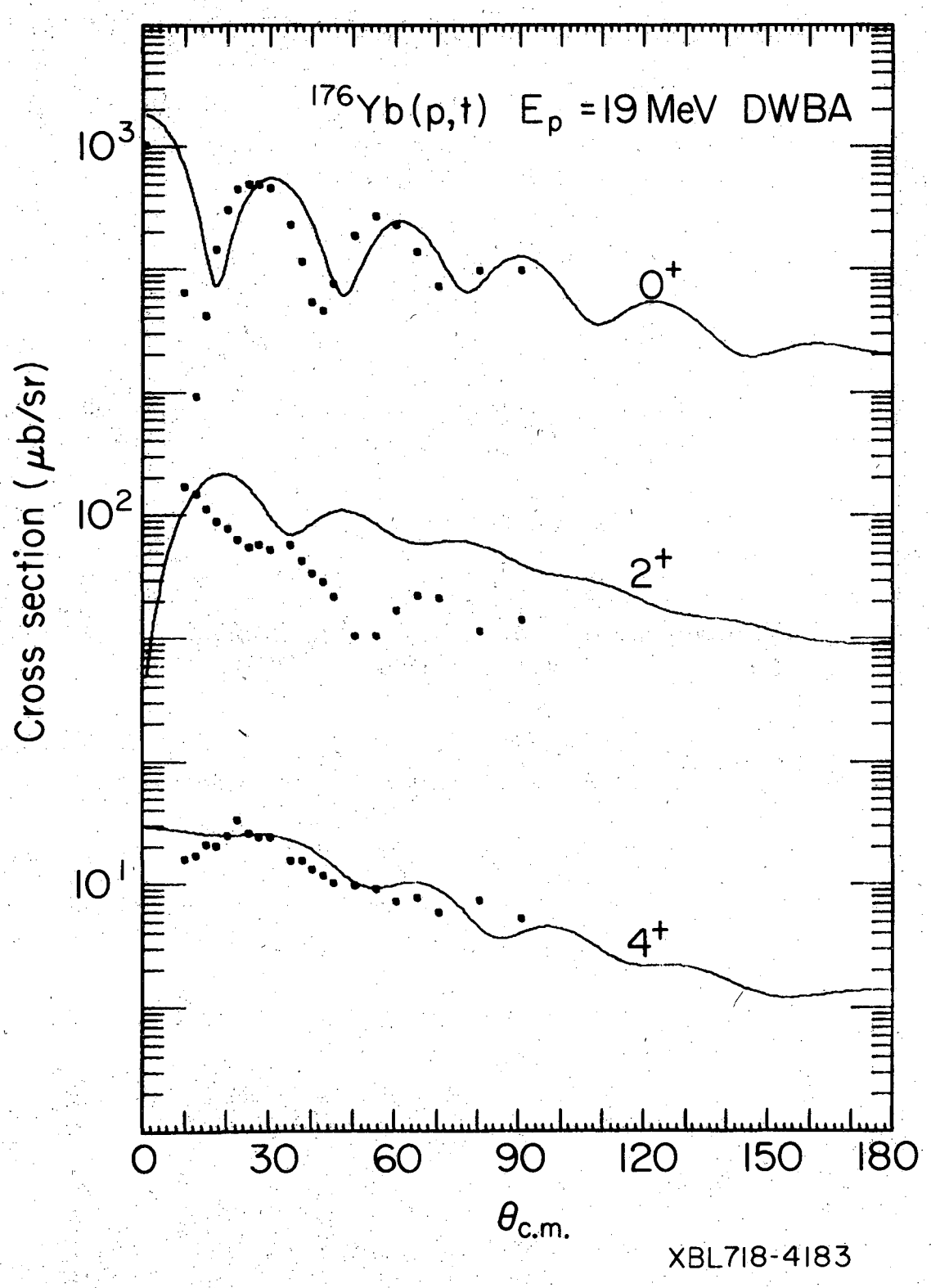

Fig. 3. DWBA cross sections normalized to the ground state leading to members of the ground band. Optic parameters were adjusted to reproduce the elastic cross sections for proton and triton obtained in the coupled-channel calculations reported subsequently (see Table 2).

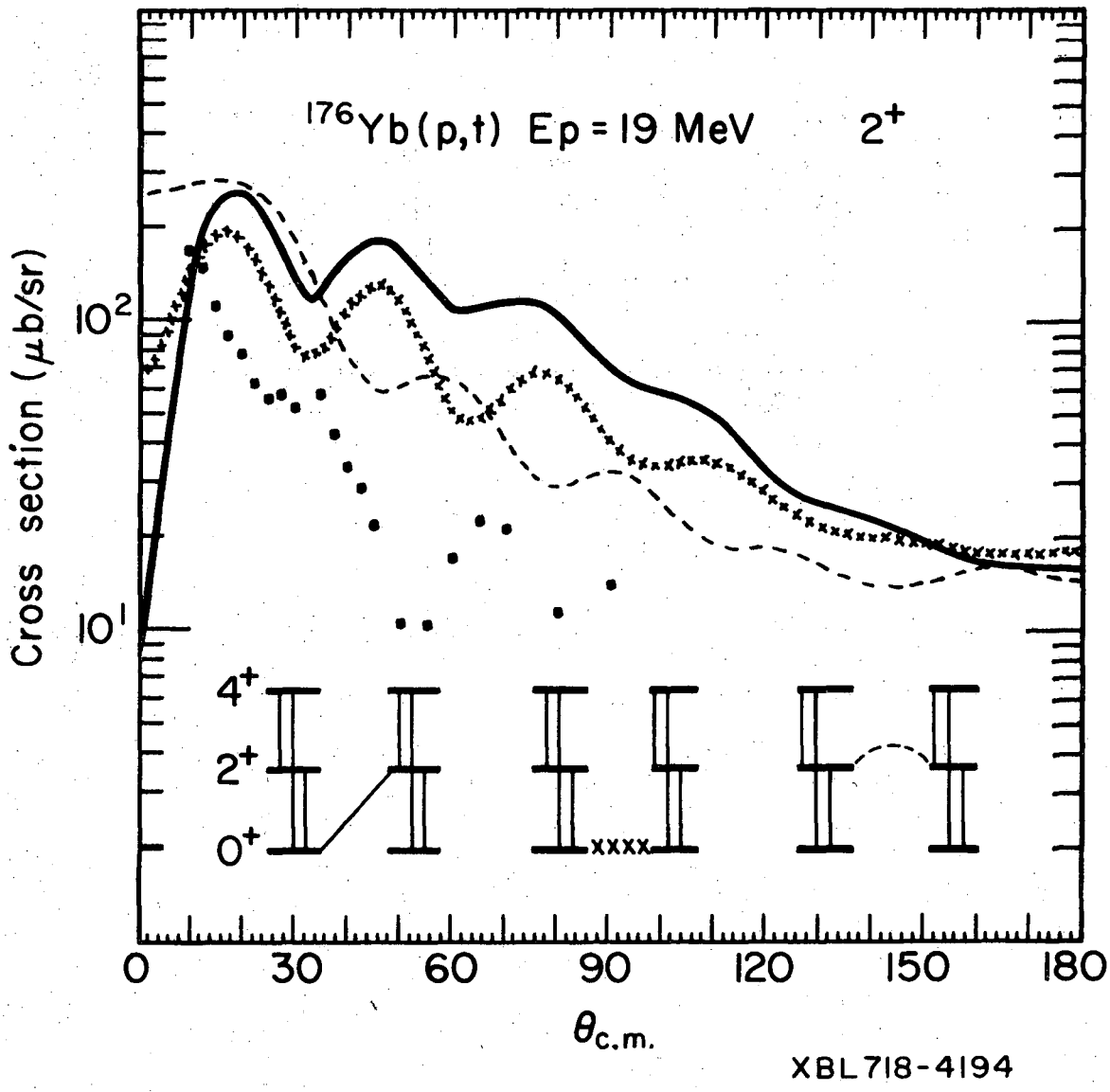

Fig. 4. Cross sections for the 2^+ state that correspond to the individual transfer processes shown. Note that the direct and indirect routes are comparable in magnitude. The normalization is the same as used in the complete calculation of fig. 5, which means that these routes each overestimate the cross section and interfere destructively to produce the final result.

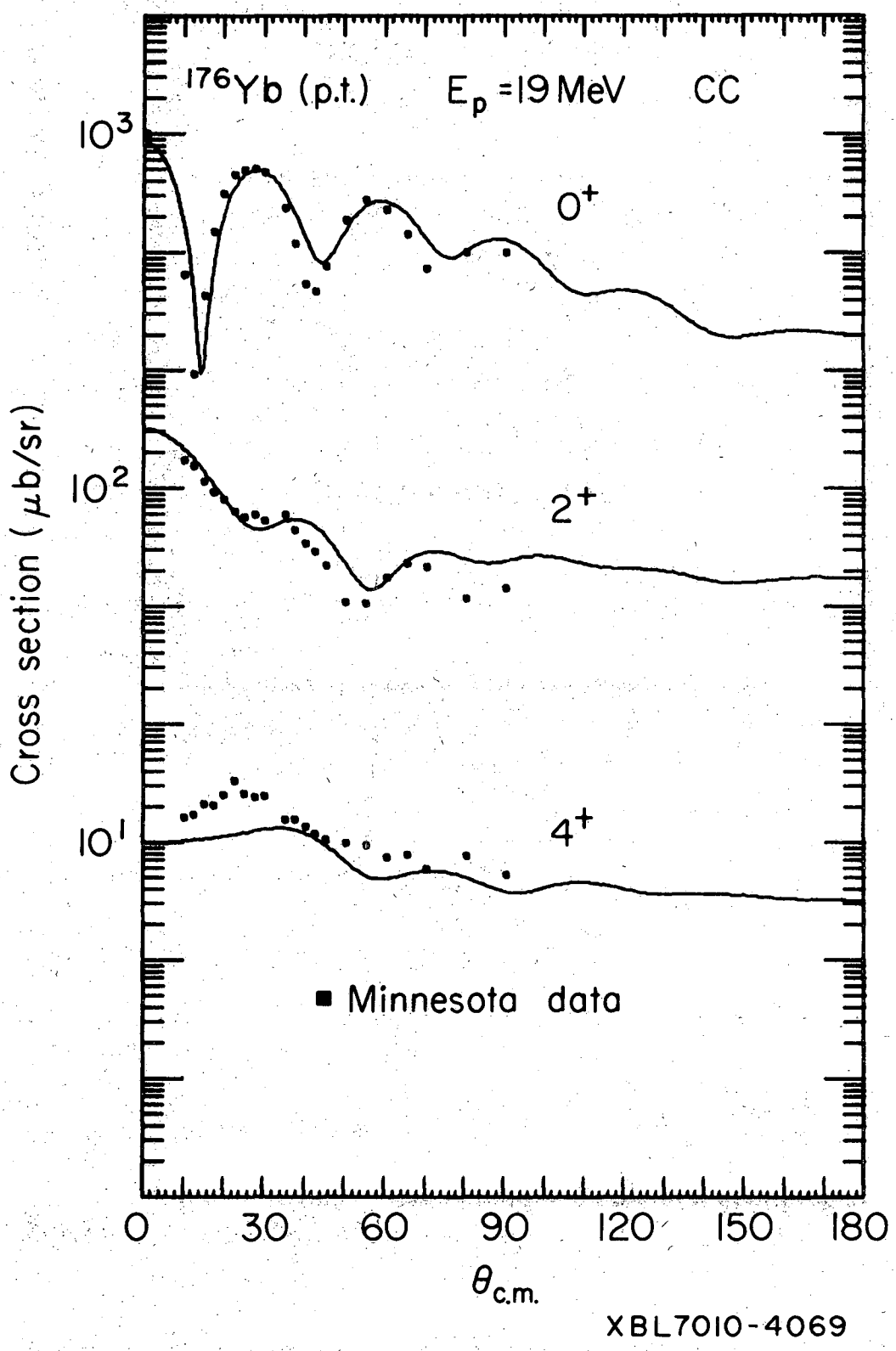

Fig. 5. Cross sections for members of the ground band of ^{174}Yb. Calculations include all transitions connecting all three states in both nuclei. The 0^+ curve was normalized to the data and the same normalization was used for the other two.

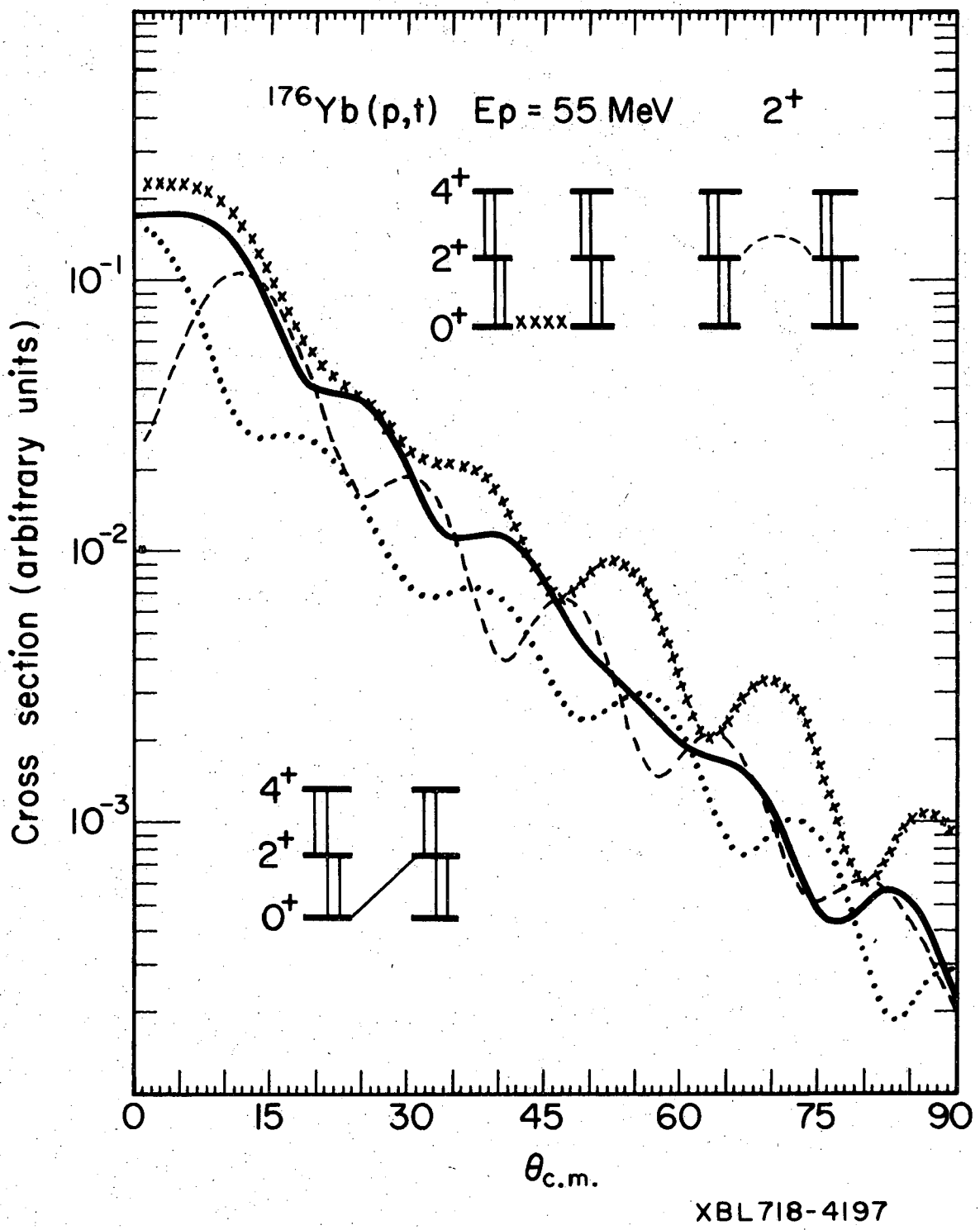

Fig. 6. Cross sections at 55 MeV for the 2^+ state that correspond to the individual transfer processes shown. The dotted curve is the resultant complete calculation, which since it is smaller than the others, shows that the interferences among the various processes is destructive.

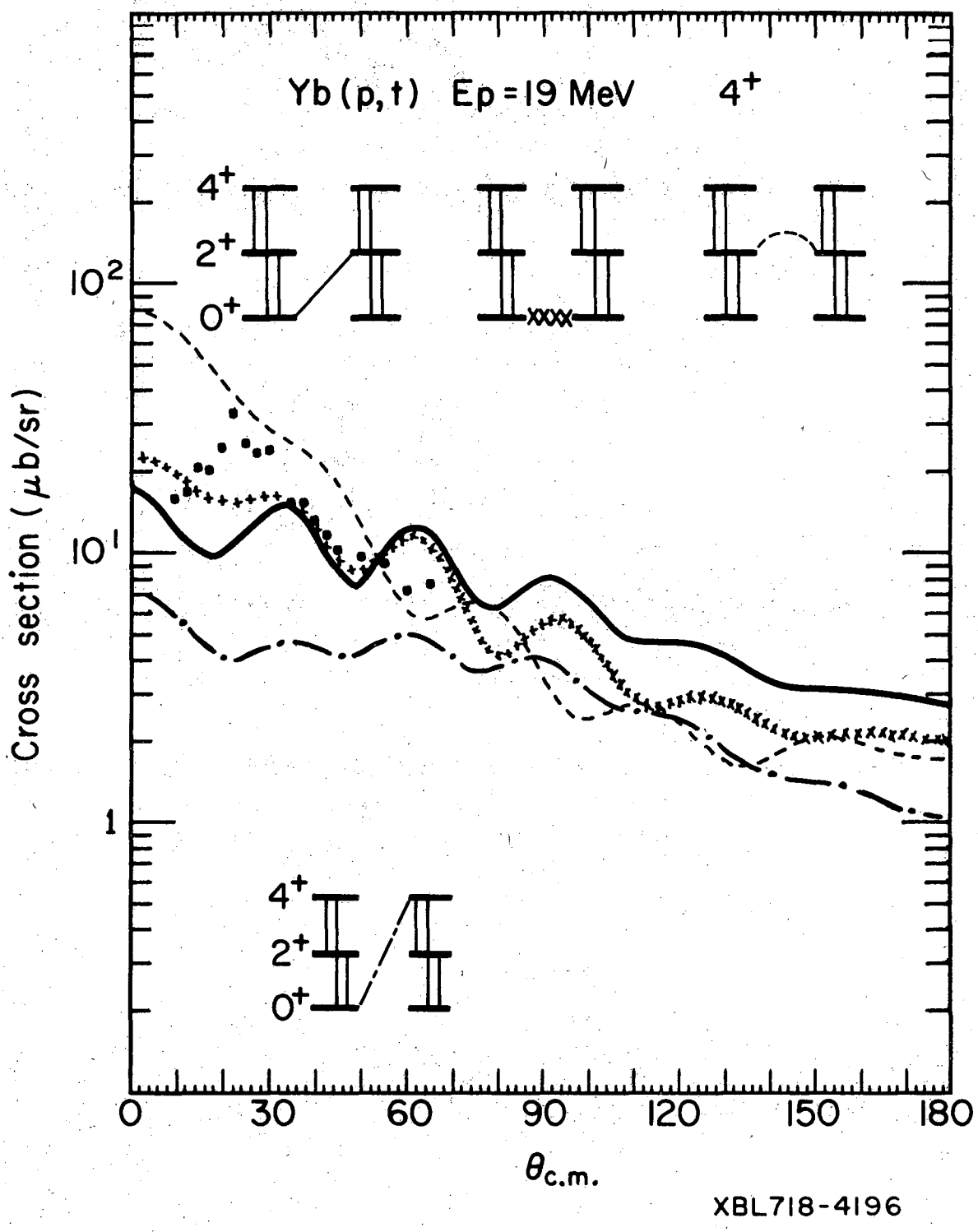

Fig. 7. Cross sections for the 4^+ state at 19 MeV corresponding to several of the many individual transfer processes.

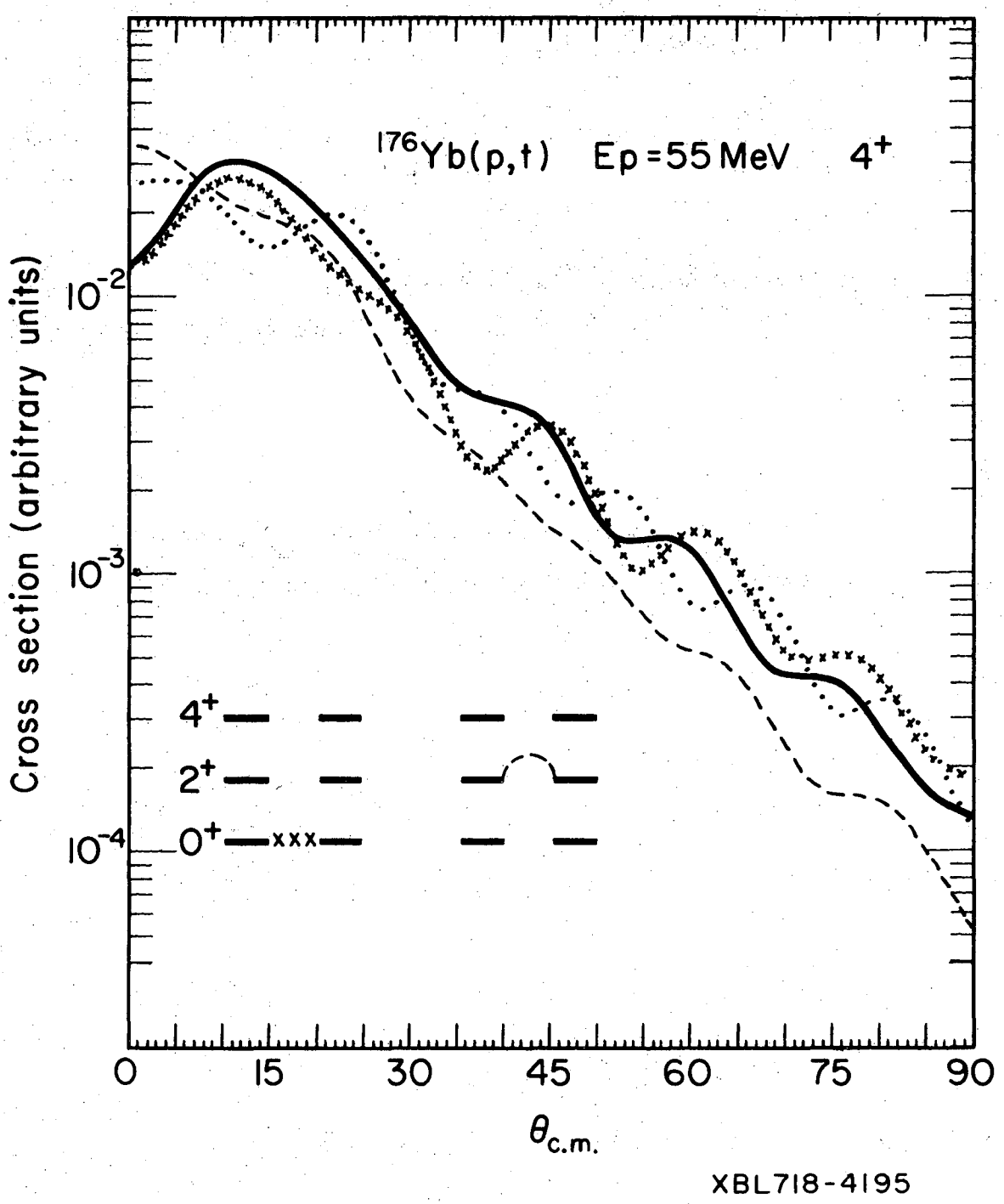

Fig. 8. Same caption as for fig. 7 but for 55 MeV. The dotted curve is the complete calculation containing the coherent contribution from all routes feeding the 4^+ state.

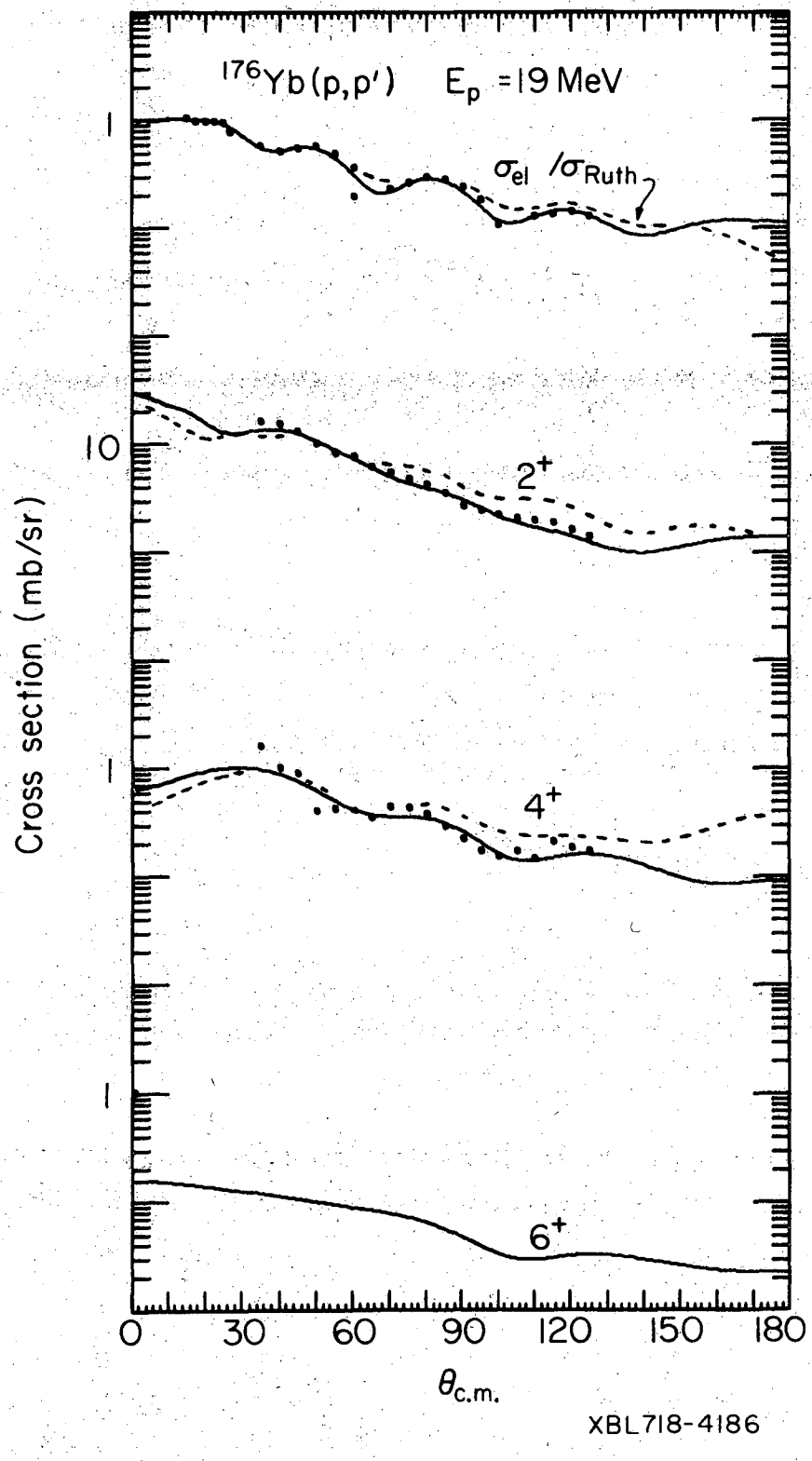

Fig. 9. Elastic and inelastic proton cross sections on ^{176}Yb at 19 MeV. The solid lines are parameters due to Hintz and the dashed are average parameters of Becchetti and Greenlees (see Table 2).

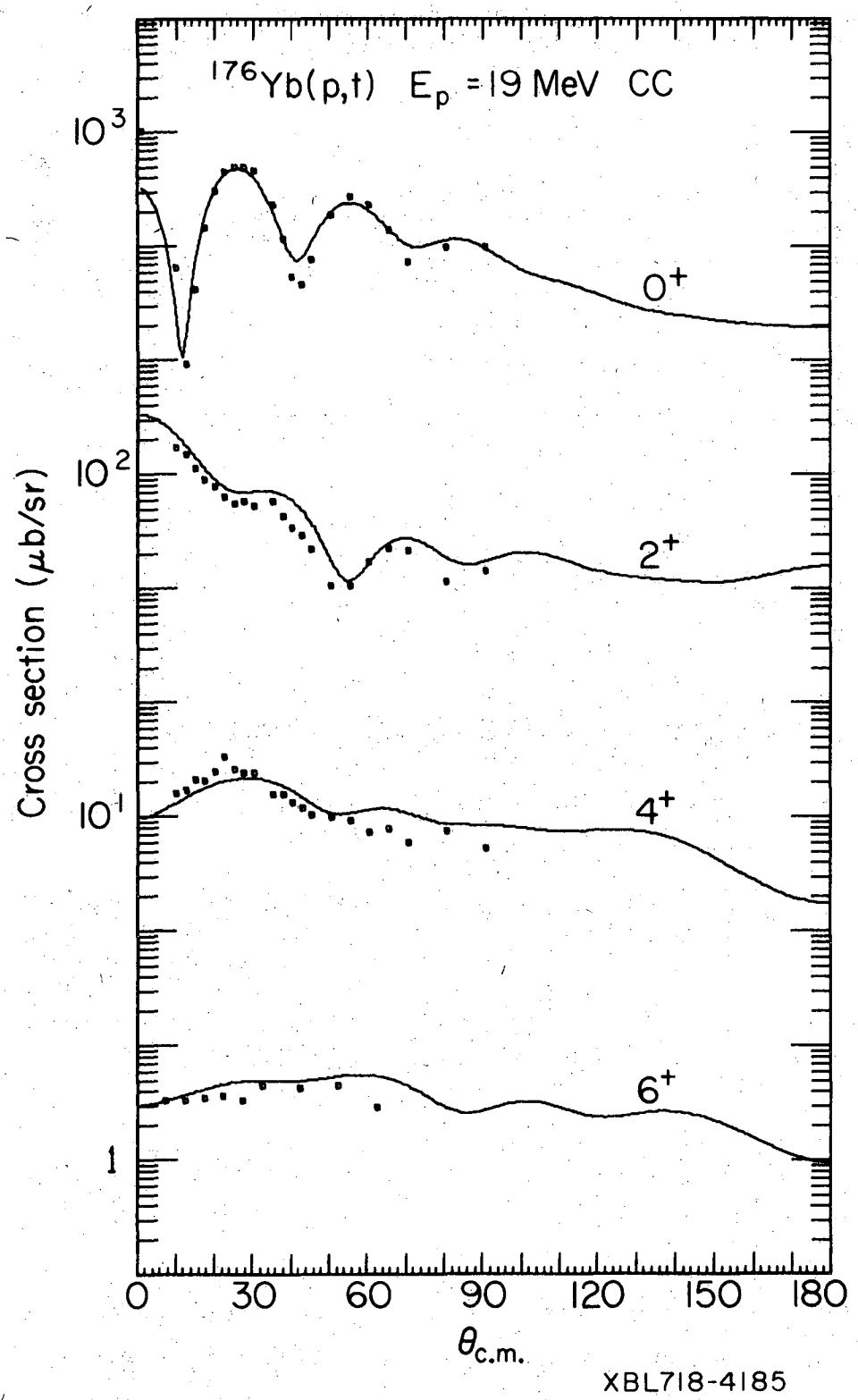

Fig. 10. Complete calculation for the ground band members of ^{174}Yb produced in the (p,t) reaction. Calculations include all inelastic and reaction transitions connecting all four states in both nuclei. The 0^+ is normalized to the data and the same normalization was used for the others. The experimental values β_2, β_4, β_6 were used as discussed in the text.

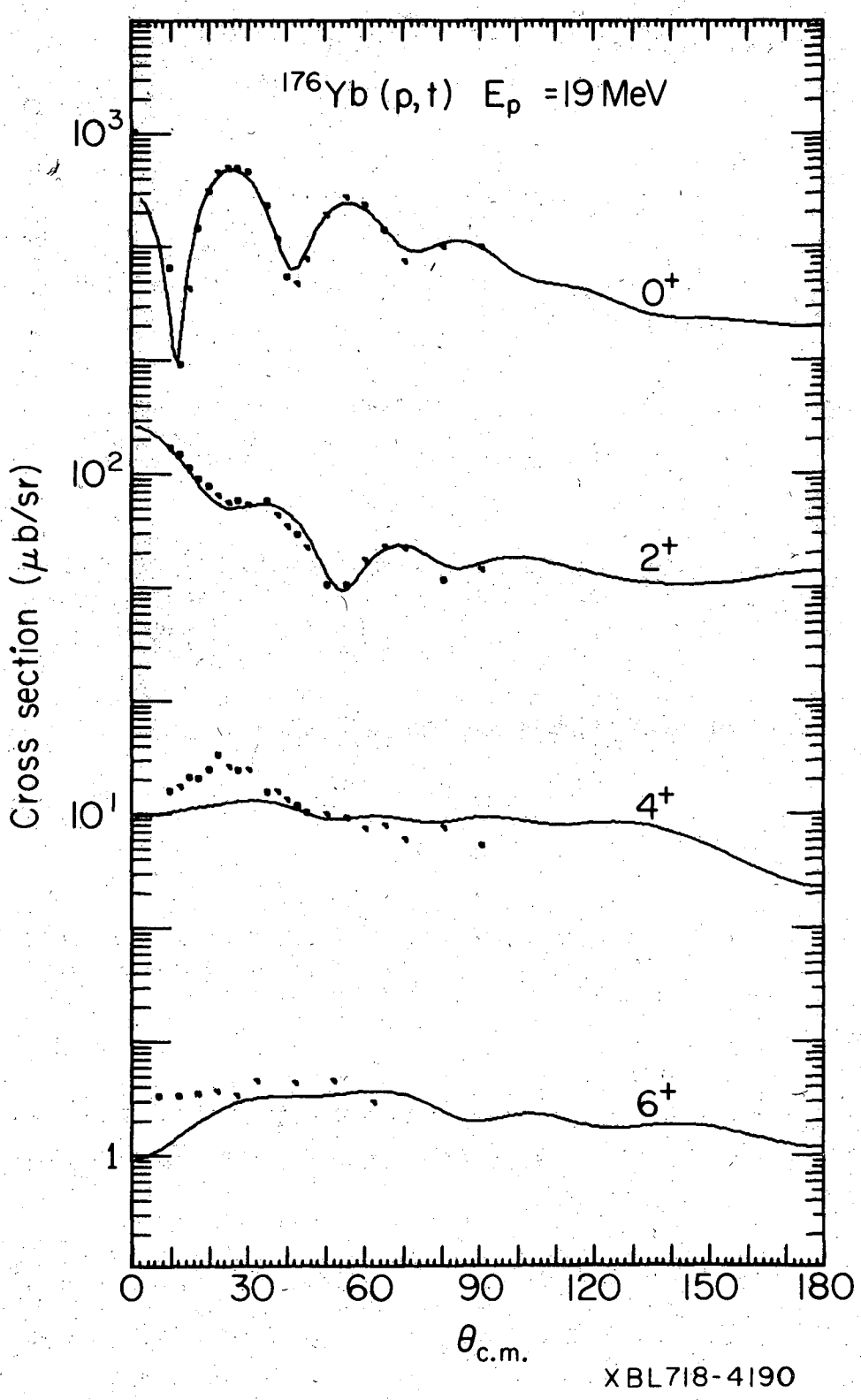

Fig. 11. Computed cross sections corresponding to $\beta_4 = \beta_6 = 0$ and β_2 adjusted to give the same quadrupole moment as for fig. 10. This illustrates the weak sensitivity to β_4 and β_6.

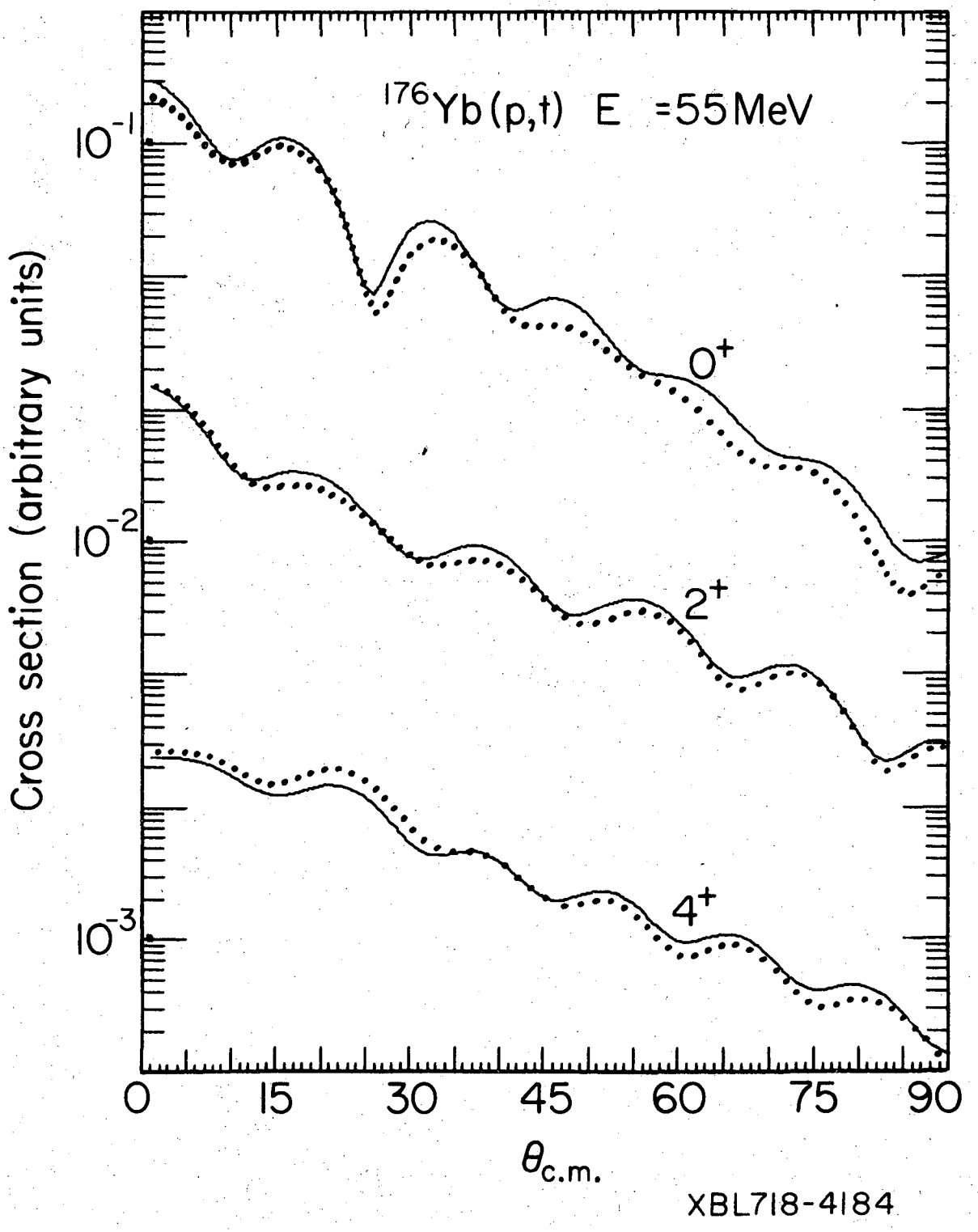

Fig. 12. Compares at 55 MeV the effect of β_4 and β_6 on the (p,t) reaction. The dotted curve corresponds to experimental values of β_2, β_4, β_6 and the solid curve to $\beta_4 = \beta_6 = 0$ and β_2 adjusted to yield the same quadrupole moment as previously.

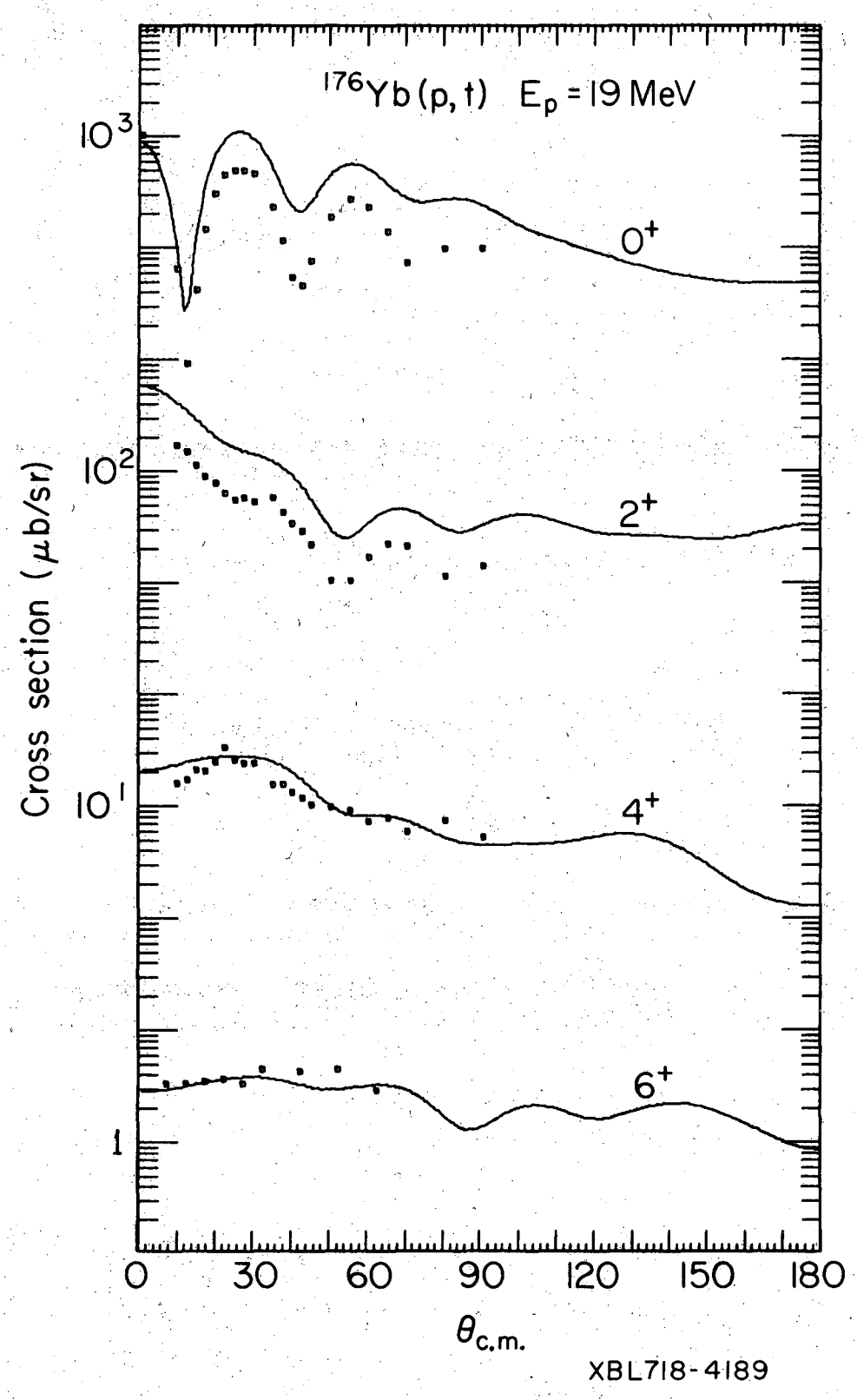

Fig. 13. The structure of the intrinsic state is here computed using 40 levels around the Fermi surface as compared with fig. 10 where 20 levels were used. The same normalization is used for the curves of both figures.

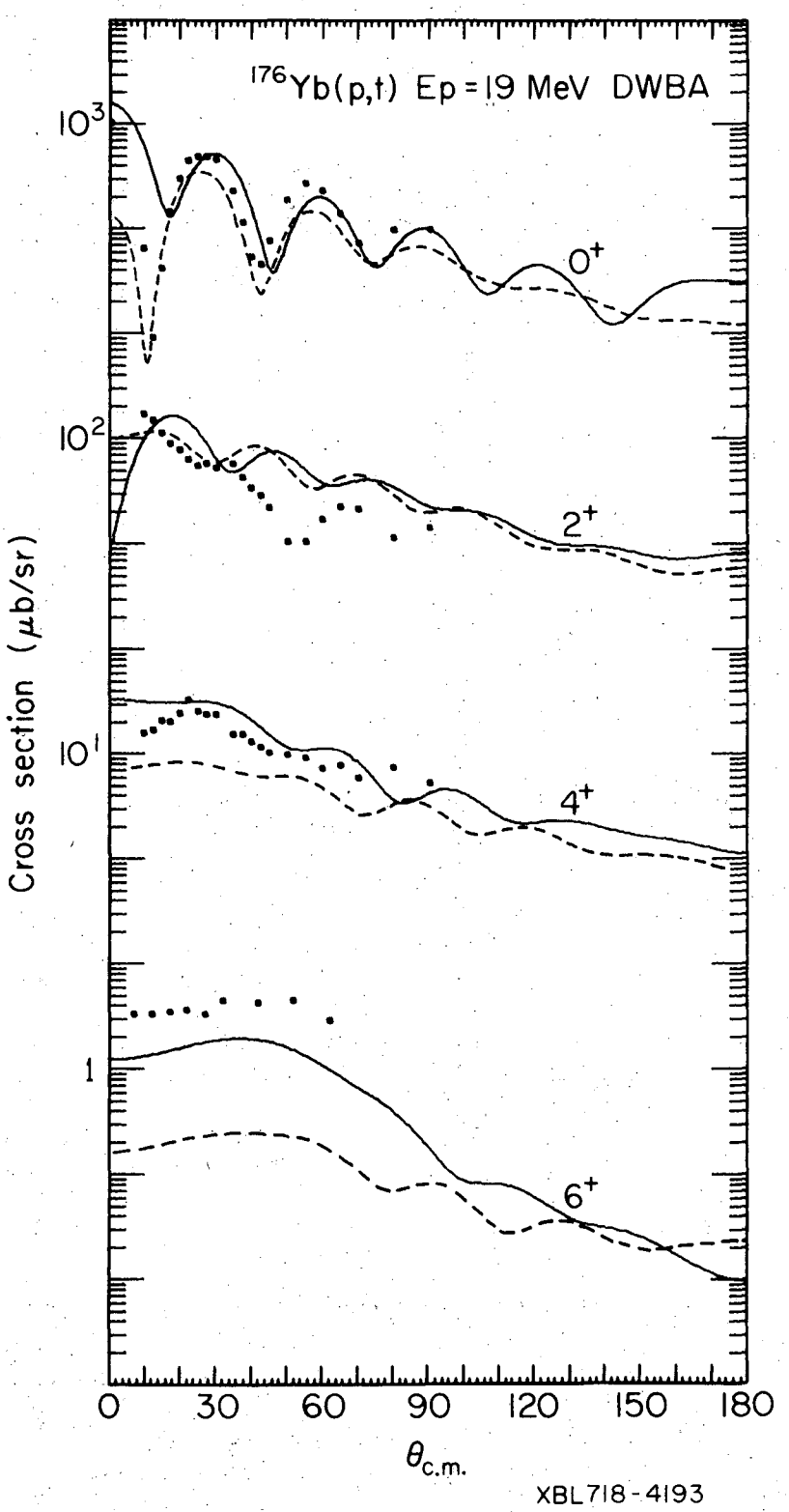

Fig. 14. Two DWBA calculations are shown. The solid curve corresponds to proton and triton parameters adjusted to reproduce the elastic cross sections of the coupled-channel calculation (shown for protons in fig. 9). The dashed curve uses the same parameters as for the coupled-channel calculation. The two sets of curves have the same normalization, which is reduced by a factor of three from the complete calculation shown in fig. 10.

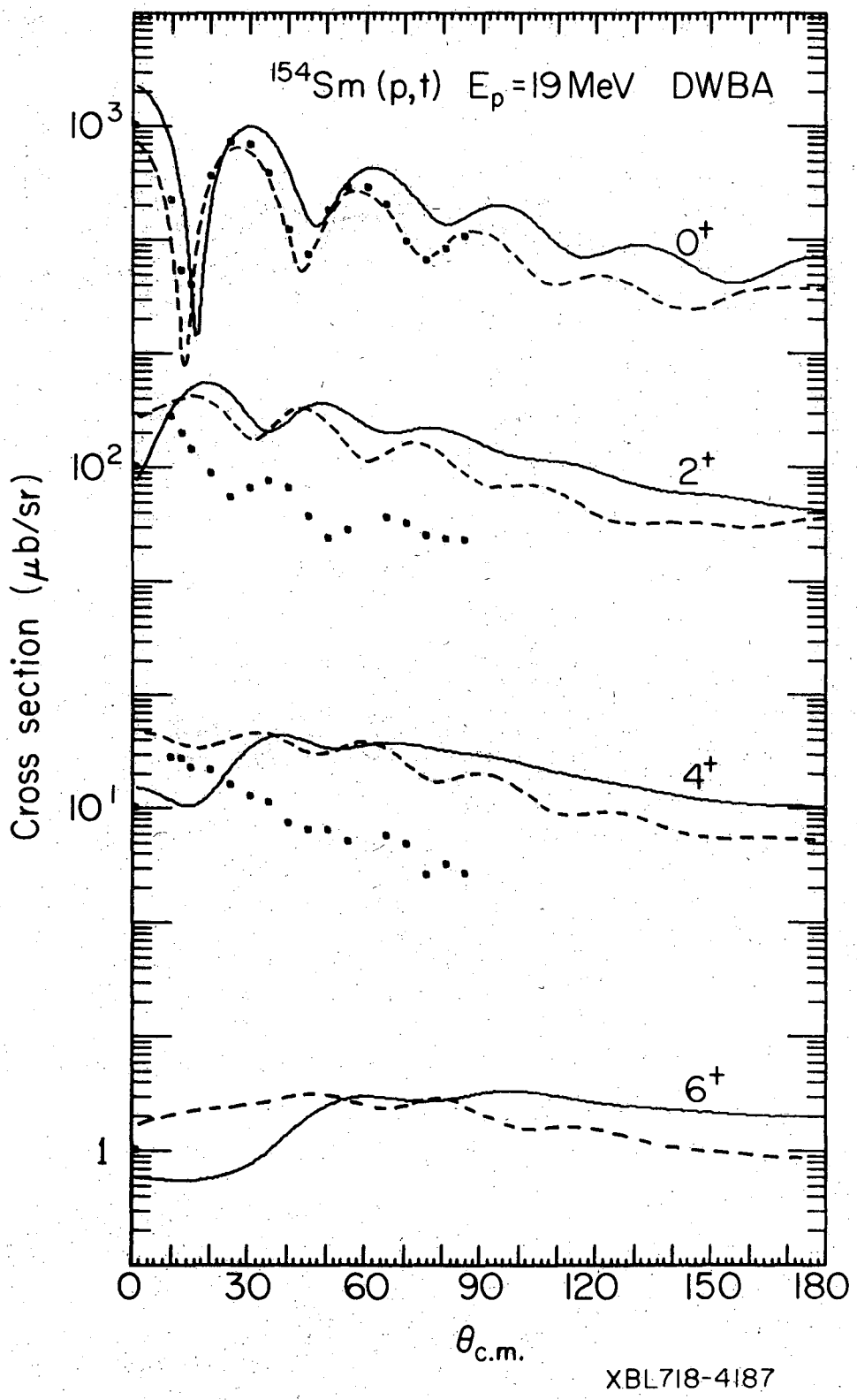

Fig. 15. Two DWBA calculations are shown. The solid curve corresponds to proton and triton parameters adjusted to reproduce the elastic cross sections of the coupled-channel calculation. The two sets of curves have the same normalization, which is reduced by a factor of 2.5 from the complete calculation shown in fig. 16.

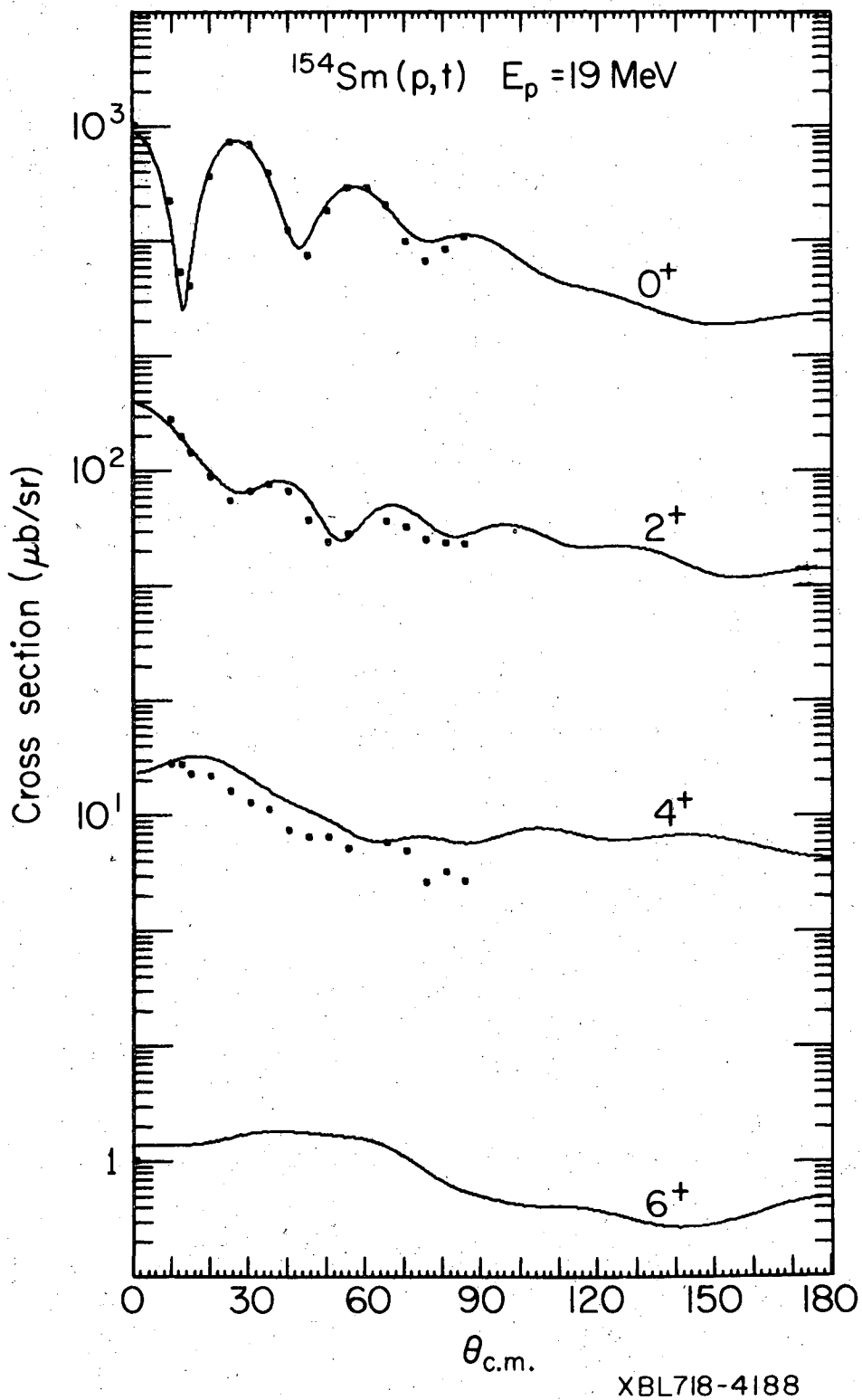

Fig. 16. Complete calculation for the ground band members of ^{152}Sm produced in the (p,t) reaction. Calculations include all inelastic and reaction transitions connecting all four states in both nuclei. The 0^+ is normalized to the data and the same normalization was used for the others. The experimental values of β_2, β_4, β_6 were used as discussed in the text.

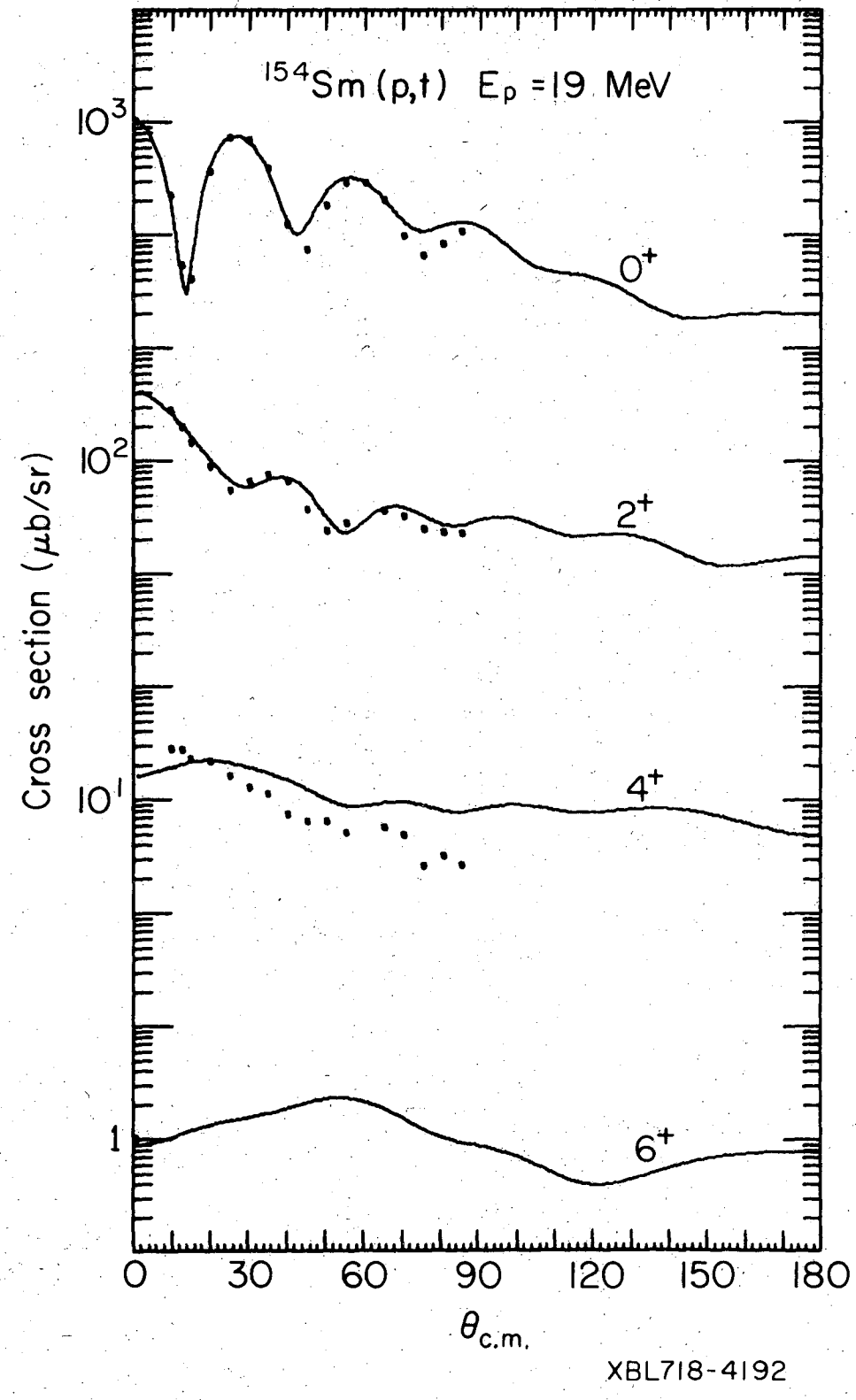

Fig. 17. Compare with fig. 16 where her $\beta_4 = \beta_6 = 0$ and β_2 adjusted to yield about the same strength in the 2^+ inelastic transition.

TECHNICAL INFORMATION DIVISION
LAWRENCE RADIATION LABORATORY
UNIVERSITY OF CALIFORNIA
BERKELEY, CALIFORNIA 94720